Published on Marine Geology 276 (2010) 42-57

A unique 4000 yrs long geological record of multiple tsunami inundations in the Augusta Bay (eastern Sicily, Italy)

De Martini P.M. [a,*], M.S. Barbano [b], A. Smedile [a], F. Gerardi [b], D. Pantosti [a], P. Del Carlo [c], C. Pirrotta [b]

[a] Istituto Nazionale di Geofisica e Vulcanologia, Sezione Sismologia e Tettonofisica, Via di Vigna Murata 605, 00143 Roma, Italy

[b] Dipartimento di Scienze Geologiche, Università di Catania, Corso Italia 55, 95129 Catania, Italy

[c] Istituto Nazionale di Geofisica e Vulcanologia, Sezione di Pisa, Via della Faggiola 32, 56126 Pisa, Italy

* Corresponding author: demartini@ingv.it, Istituto Nazionale di Geofisica e Vulcanologia, Sezione Sismologia e Tettonofisica, Via di Vigna Murata 605, 00143 Roma, Italy. Fax: +39 06 51860507, Ph. +39 06 51860546

Abstract:

We present the geological evidence for a 4000 yrs long record of multiple tsunami inundations along the coast of the Augusta Bay (eastern Sicily) and discuss its implications. The research was carried out through a multi-theme approach which benefited of an extraordinarily long historical record that we

used to guide detailed geomorphologic and geologic surveys, coring campaigns and laboratory analyses. Two sites, named the Augusta Hospital and Priolo Reserve, were selected and investigated in detail along the 25 km-long coastline of the Augusta Bay. We found evidence for six (possibly seven) tsunami deposits; three of them may be tentatively associated to the 1693 and 365 AD Ionian Sea historical tsunamis and to ~3600 BP Santorini event. The other three (possibly four) deposits are evidence for unknown paleo-inundations dated at about 650-770 AD, 600-400 BC and 975-800 BC (at Augusta Hospital site), and 800-600 BC (at Priolo Reserve site). We use these ages to extend further back the historical record of tsunamis available for this coastal area. The exceptional number of tsunami deposits found with this study allowed us to derive an average geologic tsunami recurrence interval in the Augusta bay of about 600 years for the past 4 ka. Conversely, the historical tsunami data for the past millennium suggest an average tsunami recurrence interval of about 250 years. This difference in the average recurrence intervals suggest that only the strongest inundations may leave recognizable geological signatures at the investigated sites (i.e. the evidence for the 1908 and 1169 tsunamis is missing) but also that the geomorphological setting of the site and its erosional/depositional history are critical aspects for the data recording. Thus, an average recurrence interval derived from the geological record should be considered as a minimum figure.

The identification and age estimation of tsunami deposits represent a new and independent contribution to tsunami scenarios and modeling for coastal hazard assessment in Civil Protection applications. Furthermore our study cases

provide new elements on tsunami deposit recognition related to exceptionally large events occurred in the Aegean Sea.

Keywords: 1693, 365 AD Crete, Santorini tsunamis; tsunami deposits; micropaleontology; tephrostratigraphy.

1. Introduction

The importance of prevention plans based on realistic inundation scenarios was dramatically highlighted by the Indian Ocean tsunami of 26 December 2004. These scenarios are generally based on numerical models of tsunami wave propagation (i.e. Lorito et al., 2008 and references therein) that can become more realistic and effective when calibrated with the distribution of true inundated locations and the frequency of event occurrence. This information is generally acquired by historical records but we believe that it can be properly and fully obtained also from geological investigations (Atwater and Hemphill-Haley, 1996; Hutcinson et al., 1997; Pinegina and Bourgeois, 2001, Jaffe and Gelfenbaum, 2002, Fujiwara and Kamataki, 2008). In fact, the historical records, strongly depending on the settlement evolution and on the availability of written sources in inhabited coastal areas, are usually limited to the past few hundreds of years (in Italy, although the historical dataset is exceptionally long, reliable information concerns the past millennium, see Tinti et al., 2007 and references therein) and thus represents an incomplete set of possible tsunami inundations. Conversely, geological evidence for tsunami related deposits can furnish a longer record extendible back in time for the past 5-6 ka, providing that the present coastline and the sea level were relatively stable since then. The knowledge of the distribution and characteristics of tsunami deposits can help to answer questions about where a tsunami inundation can take place in the future, how big it can be and how often it can occur (Fujiwara and Kamataki, 2008; Pignatelli et al., 2009). In the past twenty years several geological studies provided the exact location, distribution and age range of inundations through the recognition and dating of paleotsunami deposits (Atwater and Moore, 1992; Dawson et al., 1995; Pinegina et al., 2003; Cochran et al., 2005, Dominey-Howes et al., 2006; Nichol et al., 2007; Nanayama et al., 2007, Bruins et al., 2008; Sheffers et al., 2008; Shiki et al., 2008 and references therein). However, because of the limited number of events found in a specific region (generally one or two tsunami deposits), only rarely an average tsunami recurrence interval was derived. In Italy, tsunami geology began no more than 10 years ago. The first work describing tsunami deposits focused on the Gargano coast (Adriatic Sea side) and highlighted deposits possibly related to the 1627 tsunami and to previous ones occurring with a recurrence interval of about 1700 years (De Martini et al., 2003). In the same area, washover fans in the Lesina coastal barrier were interpreted as an effect of tsunami waves (Gianfreda et al., 2001). More recently, tsunami deposited layers were recognized in an archaeological excavation in the NE tip of Sicily (Pantosti et al., 2008). Other tsunami geology studies concern the transport and deposition of large boulders scattered along the coasts of Apulia (Mastronuzzi and Sansò, 2000; 2004; Mastronuzzi et al., 2007) and of southeastern Sicily (Scicchitano et al., 2007). Because eastern Sicily was affected in historical times by large earthquakes (CPTI Working group, 2004) followed by devastating tsunamis (Tinti et al., 2007), we selected this region to develop a multi-disciplinary study designed to search for geological evidence of historical and paleo-tsunami deposits. Along the eastern Sicily coasts, we selected the Augusta Bay as the key area of this study because it is one of the locations where both information available from historical written reports on tsunami effects (hit localities, inundated areas and run-up distribution) and local geomorphology suggest it is very favorable for the research of the geological signature of past tsunamis.

In this paper we present the geological evidence of paleotsunami deposits found at two different sites, namely the Augusta Hospital and Priolo Reserve, located in a marsh/lagoonal environment, about 10 km apart along the Augusta Bay coast (Fig. 1a). We also discuss the implications related to this unique case of recognition of multiple inundation events. This research was carried out during the past four years and involved historical studies, geomorphologic and geological surveys, coring campaigns, and several laboratory analyses (paleontological, radiometric, X-Ray, magnetic susceptibility, tephra, etc.).

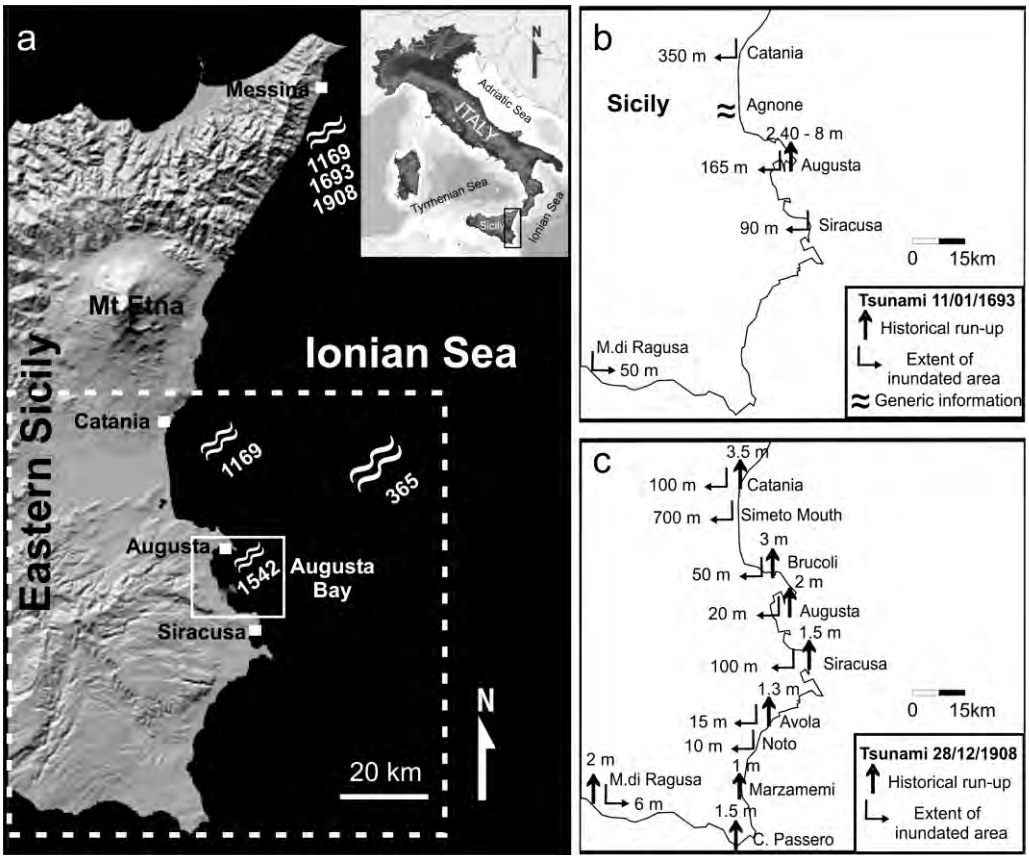

Fig. 1 – a) Location of the Augusta Bay area and generic historical tsunami data; b) and c) detailed run-up and inundation data for the 1693 and 1908 tsunamis, respectively, in the Augusta Bay area and surroundings.

2. Historical Tsunamis in southeastern Sicily

Because of the wealth of historical data available on the effects of tsunamis in the past millennium, eastern Sicily represents an exceptionally favorable case for collecting, organizing and analyzing data on these events. In the following we summarize the available data (Fig. 1) for the southeastern Sicilian coast, with particular emphasis on the Augusta Bay area. Original text of historical sources together with other reports are available as supplementary material in Appendix A.

July 21 365

Historical seismic catalogues (Guidoboni et al., 1994; Papazachos and Papazachou, 1997) affirm that one of the most impressive earthquakes of ancient times hit Crete in 365 AD, generating a tsunami that affected the coasts of the entire eastern and central Mediterranean. More specifically, Jerome (380) attests that in 365 AD there was an earthquake throughout the World, and that the sea flowed over the shore, causing suffering to countless people in Sicily and many other islands.

February 4, 1169

This tsunami followed a local earthquake, with estimated magnitude $M_{aw} = 6.6$ (M_{aw} = average weighted Magnitude derived from macroseismic intensities, CPTI Working group, 2004) and inundated the shore between the town of Messina and the Simeto river (its mouth is located about 20 km N of Augusta town and 10 km S of Catania town). In the Messina town waves overcame the city walls, inundating the streets (Fazello, 1560). Mongitore (1743) reports that "the earthquake caused 25000 victims and many other were killed by the sea waves rising along the whole shore of the island".

December 10, 1542

This earthquake, with estimated magnitude $M_{aw} = 6.6$ (CPTI Working group, 2004), hit many localities in south-eastern Sicily causing damage in an area of about 6000 km^2 (Boschi et al., 2000). Several localities were destroyed and the shock was felt in whole the island (Barbano and Rigano, 2001). As reported by Lacisio (1543) that wrote "Sicily was shaken by an earthquake so big and so horrible that … Augusta was almost all flooded by the sea", after the earthquake the sea flooded the town of Augusta.

January 9 and 11, 1693

In 1693 two big earthquakes ($M_{aw} = 6.2$, January 9, and $M_{aw} = 7.4$, January 11, according to CPTI Working group 2004) caused destruction and heavy damage in most of the localities of eastern Sicily. After the mainshock a large tsunami affected the whole eastern coast of Sicily, the Aeolian Islands and Mazzarelli, the old Port of Marina di Ragusa (Campis, 1694), in the southern Sicilian coast

(Fig. 1b). The known length of inundated shoreline was of about 230 km (Gerardi et al., 2008). For the January 11 tsunami, the sea flooded the Catania town, inundating San Filippo square (now Mazzini square) and the neighbouring farms. In the Siracusa town the sea withdrew about 50 steps and then overran the shore (Boccone, 1697). More specifically, concerning the town of Augusta, the sea withdrew completely from the harbour and then violently came back over-passing the coastline of about 30 cubits (~ 165 m) (Bottone, 1718) and inundated the city as far as the San Domenico Monastery (Boccone, 1697). According to a contemporary witness also the January 9 event was followed by a tsunami: "the January 9 in the night, about 5 o'clock (Italian local time corresponding to about 21 GMT), the persons standing in the Augusta harbour were hit by raging sea waves and by their unusual motions" (Campis, 1694).

- *December 28, 1908*

The 1908 Messina earthquake (M_w = 7.1, Pino et al., 2000) is the most catastrophic event occurred in the 20th century in Italy; it produced extensive destruction over an area embracing southern Calabria and north-eastern Sicily (Boschi et al., 2000 and references therein). A tsunami violently hit the southern Calabrian and the eastern Sicilian coasts causing further damage and causalities (Platania, 1909; Sabatini, 1910). The tsunami wave was also observed along the Tyrrhenian coast of Sicily and in the Sicily Channel as far as the Malta Islands (Platania, 1909; Baratta, 1910). The known length of inundated Sicilian shoreline was at least 270 km (Gerardi et al., 2008).

The tsunami flooded inland up to 250 m in north-eastern Sicily (Platania, 1909). In the Messina town the tsunami inundated the harbour-office and the St. Salvatore fortress (Platania, 1909). The waves flooded the town of Catania (Fig. 1c) for more than 100 m inland depositing algae, posidonie, madrepore and millepore fragments, molluscs and many dead fishes; the shore was overflowed for about 700 m inland at the mouth of the Simeto river (Baratta, 1910). In Siracusa, after the withdrawal, the wave raised about 2 m, the water covered the banks and only some boats were damaged (Baratta, 1910). Detailed information exists for Brucoli village, less than 10 km N of Augusta town, where 8 minutes after the shock the sea withdrew for more than 200 m, then the sea flooded for about 50 m inland depositing boats, small fishes, echinoderms, crabs (Platania, 1909). In the Augusta city "around 20 minutes after the shock, a rumpus similar to that produced by the waves braking against rock-cliffs was felt inside the harbor; after a few seconds the sea flooded the beach with a series of waves, the greatest of which was the first one and raised to 1.75 m. The duration of this phenomenon was about 10 minutes, but later, for the whole day waters remained shaken. Out of the harbor the waves raised over 2 meters and propagated onshore for about 15 meters. The tsunami damaged the Augusta town Salt pan (Baratta, 1910).

Summarizing, the investigated area experienced at least four tsunamis (in 1908, 1693, 1542 and 1169) during the past millennium (period for which we believe that the historical tsunamis record can be considered complete, at least for the main events). As already known from the Italian seismic historical catalogues, the Middle Age period is quite scarce of information due to unstable social and economical conditions and thus the historical tsunami record is very poor before 1000 AD. However, it is well known that the large 365 AD Crete earthquake-generated tsunami hit the Augusta Bay area (Jerome, 380) as supported also by numerical modeling (Lorito et al., 2008; Shaw et al., 2008). Although aware of the difficulties in using these historical records for statistical purposes, an average tsunami recurrence interval (ATRI) of about 250 years for the past millennium in the Augusta Bay can be derived from written reports (a ~400 years long ATRI is obtained considering the ca 2 ka long historical dataset).

3. Tsunami deposits

Tsunami sedimentation can take place in both on-land and off-shore environments and since the tsunami behaviour depends strongly on bathymetric and topographic configurations, different sedimentation patterns can occur depending on the differences in these environments (Sugawara et al., 2008). Since the two sites investigated in this work are coastal marsh/lagoon areas, we mainly concentrated on tsunami deposit characteristics observed inland and in this environment. In fact, coastal lacustrine environment can provide an excellent and convenient restricted condition for recognizing and identifying tsunami deposits (Shiki et al., 2008). This environment is an excellent trap able to favour both sedimentation and preservation of tsunami sediments. Characteristic marine sand layers in coastal lagoons and lakes have been investigated worldwide and identified as records of historical and pre-historical tsunami inundations (Sugawara et al., 2008). Tsunami deposits are commonly recognized as high-energy sediments in a clearly different low-energy environment, such as a marine sand layer deposited in coastal plains, lagoons, or tidal marshes or because of the presence of open marine microfossils in shallow coastal settings (Goff et al., 2001; Scheffers and Kelletat, 2003).

In general, the tsunami deposits are sheet-like and can be locally patchy, they commonly exhibit evidence of rapid deposition, such as normal grading or massive structure, and an erosional basal contact (Clague et al., 1994; Gelfenbaum and Jaffe, 2003; Tuttle et al., 2004; Dawson and Stewart, 2007; Shiki et al., 2008). In coastal lakes or lagoons, a tsunami deposits may consist of a distinct sand layer, showing a general fining upward and fining landward trends, usually structureless (Sugawara et al., 2008). It may contain rip-up clasts, clastic and biogenic particles. The dominant organic remains and fossils from offshore, such as foraminifera, diatoms, fragments of corals and bivalves, are characteristics of run-up tsunami wave sediments (Shiki et al., 2008).

Given the high variability in the nature of tsunami sediments, it is not surprising if tsunami deposits are not uniquely identifiable, and other kinds of deposits, storm- or hurricane derived, may share most of their characteristics. Because we are looking for tsunami deposits we cannot avoid consideration about the difficulty in differentiating them from storm deposits.

Sedimentary characteristics such as layer thickness, sorting, sharp basal contacts and inland extent have been used to distinguish tsunami deposits from storm-generated sediments. In recent years, only a few studies were designed to compare sedimentological characteristics of historical tsunami and storm deposits at the same or nearby site in order to reduce sediment and landscape variability (Nanayama et al., 2000; Goff et al., 2004; Tuttle et al., 2004; Kortekaas and Dawson, 2007). Based on these studies, tsunami deposits may differ from storm deposits in terms of thickness (usually larger for storm), grain-size characteristics (storm deposits are better sorted) and internal structure (storm deposits consist of interbedded and laminated layers and may show foreset and cross-bedding while tsunami deposits are composed by one to few massive or fining upward layers). A recent review paper (Morton et al., 2007), on the physical criteria for the abovementioned distinction, uses several modern examples to describe idealized tsunami and storm deposits. The presence of a relatively thin deposit (average <25 cm) often made by normally graded sand consisting of a single (or few) structureless bed, sometimes with rip-up clasts, strongly favor a tsunami origin; on the other hand, a moderately thick sand bed (average >30 cm) composed of several planar laminations with foreset and ripples clearly favor a storm origin (Morton et al., 2007). Moreover, from a physical point of view (see Fujiwara, 2008 for a recent update on differences of waveforms between tsunami- and storm-induced waves), because high-energy tsunami waves have long wavelengths (up to some 100 km), these have the potential to travel further inland with respect to storms, as these latter have variable energy and wind-generated waves are characterized by shorter wavelengths (up to few km). Hence, tsunamis are able to deposit material well far inland with respect to storms: these latter are generally confined within 200 m from the coast (Nanayama et al., 2000; Goff et al., 2004; Tuttle et al., 2004). Even in cases of hurricanes or typhoons (not observed in historical times in the Mediterranean sea) sediment deposition is typically restricted to about 200-250 m from the shore, with few examples/sites of kilometer-scale distances (usually river valleys) to be considered rare and not representative of typical storm deposits (Morton et al., 2007). Finally, since the occurrence of storms along a coastal area is usually much more frequent than tsunamis, the tsunami deposits record in the sedimentary sequence is expected to be less numerous than the storms related one.

Thus, the geological approach may be complicated by erosion/deposition process related to storms (Morton et al., 2007) and by the possible presence of a tsunami-related erosion/bypass zone (no deposition), usually as far as 150 m inland (Gelfenbaum and Jaffe, 2003).

In order to avoid most of these problems we selected only sites wide enough to perform our coring campaigns starting from a minimum distance of 200 m from the present shoreline and moving further inland as possible.

4. Looking for paleotsunami deposits in the Augusta Bay area

The Augusta Bay area (Fig. 2) is a natural gulf, about 15 km wide and with a 25 km-long shoreline, located along the Ionian coast of the Hyblean mountain range. During the past century part of the bay has been walled up with breakwaters (about 6 km long) to form an important harbour communicating with the sea through two narrow inlets. Most of the lowlands facing the sea are presently used by important industrial petrochemical facilities and part of the harbour is a basis of the Italian Navy and NATO. The lithologies outcropping in the area, apart from Holocene and Late Pleistocene alluvial and fluvial deposits, are dominated by coarse sands, calcarenites and limestone as old as Late Cretaceous (Lentini et al., 1986)

After a preliminary detailed geomorphologic study of the Augusta Bay, through aerial-photographs, satellite images interpretation and field surveys, we concentrated our study on the sites of Augusta Hospital and Priolo Reserve (Fig. 2). At these sites marsh/lagoonal environment appeared favorable to sedimentation, preservation and dating of tsunami deposits.

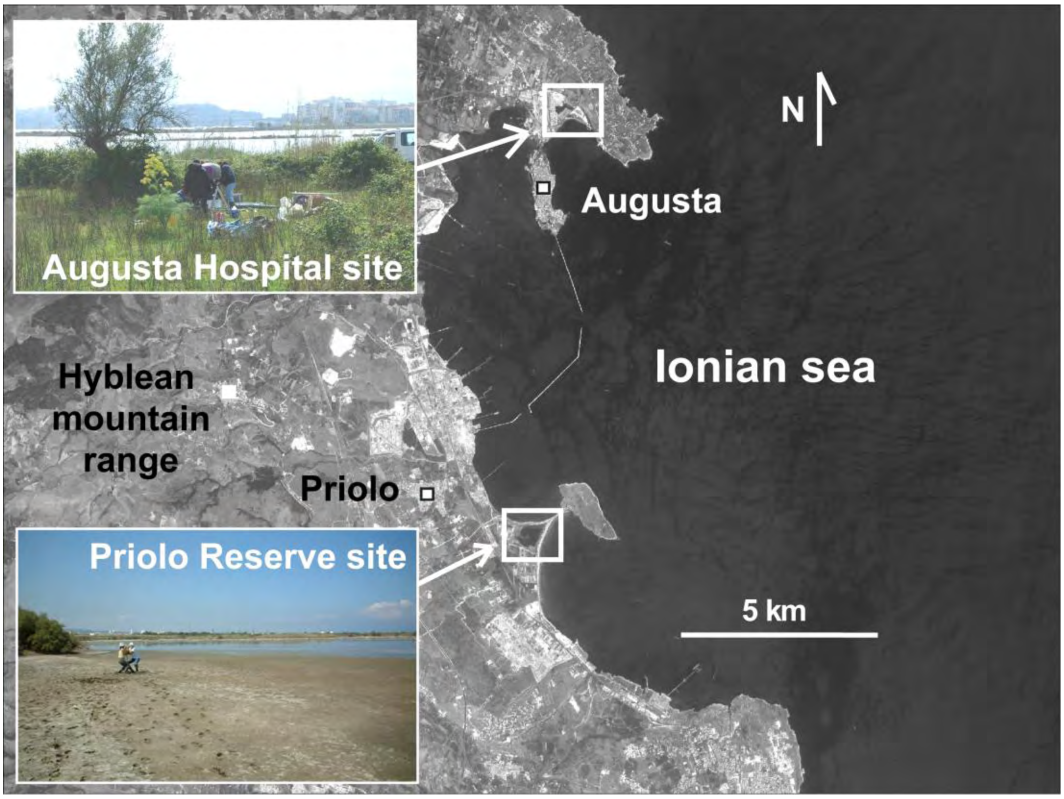

Fig. 2 – Map of the Augusta Bay area and pictures of the investigated sites. Please note that the morphology of the two sites is different (see also Figs 3 and 6), in fact the Augusta Hospital site is characterized by a gently seaward dipping surface while the Priolo Reserve site is the flat surface of the bottom of the lagoon, dried only occasionally in summer.

We carried out coring campaigns in the two selected sites using both hand auger equipment and a vibracoring (gasoline powered percussion hammer). Preliminary stratigraphical and sedimentological descriptions together with photographs of the core deposits were performed directly in the field. Once an interesting stratigraphic sequence was found we collected 1.0 m long core sample sections (within pvc tubes) down to a 5 m maximum depth. Coring was always accompanied by GPS surveys for its exact positioning with respect to the present shoreline.

Once in the laboratory, all the pvc core sections have been submitted to accurate sedimentological descriptions and sampled for paleontological and tephra analyses as well as isotopic dating. Micropalentological analyses were carried out on samples collected in all the performed cores in order to detect the possible marine component of high-energy coarse layers deposited within a marsh or lagoon sequence. In fact, micropaleontology consisted of quantitative and qualitative analyses of the benthic foraminifera assemblage. Samples containing well preserved and abundant benthic foraminifera were counted (at least 100 specimens) and identified in the size fraction <125 µm.Tephra identification and radiocarbon analyses (performed according to Calib REV5.0.2 by Stuiver and Reimer, 2005) were used to constrain the age of the sediments, to derive sedimentation rates and to correlate marine inundation deposits with historical tsunami events. Magnetic and X-ray analyses were performed on some selected cores to look for magnetic susceptibility variations and peculiar small-scale sedimentary structures (e.g. sharp contacts, convoluted layers, etc.)

usually not clearly detectable through the standard stratigraphic analysis. Each marine inundation deposit has been numbered from the top with a site label and a progressive number (e.g. AU-01, PR-04, etc.).

4.1 The Augusta Hospital site

The Augusta Hospital site (Fig. 2) is located to the NE of the bay, in a small inlet delimited to the W by the N-S trending island where the old Augusta town was built. It is placed on an alluvial surface (1 to 5 m a.s.l.) gently dipping to the SW, towards a large salt marsh (0.3 km^2) bounding the sea. In this site we dug 6 cores down to a maximum depth of 4.3 m and at a maximum distance of 460 m from the sea (Fig. 3).

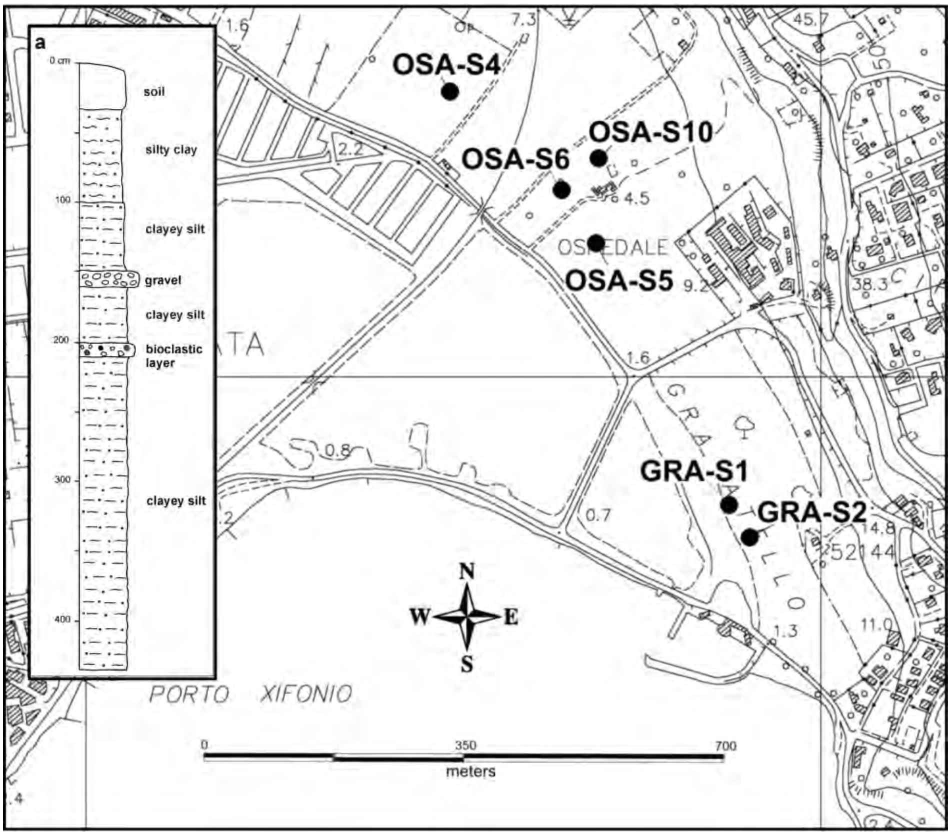

Fig. 3 – Detailed map of the Augusta Hospital site (based on the Regional Technical Cartography, RTC, 1:10000 scale); black dots represents cores

location. On the left, schematic stratigraphic log of the sedimentary sequence found at this site.

The site stratigraphy, being related to an alluvial environment, is characterized by lateral changes that occur even within a few hundreds of meters. By merging the stratigraphy from all the cores a simplified sequence can be derived (from bottom to top) as follows (Fig. 3a): 1) about 4.3-1.0 m depth thick dark brown to gray clayey silt to silt layers, with sparse/rare pebbles (strongly weathered in the lowermost 2 m), rich in vegetal remains and shell fragments between 2 and 1 m depth, interrupted at about 2 m depth by one ~ 8 cm thick peculiar bioclastic deposit and at about 1.5 m depth by one ~ 10 cm thick gravel layer; 2) about1.0 - 0.3 m depth brown to hazel silty clay to clayey silt layers with sparse calcarenites clasts (only locally organized in small lenses 1-3 cm thick), small macrofossils fragments and vegetal remains deposited; 3) about 0.3 m -top thick dark brown agricultural, plowed soil, with several roots, sparse and small pebbles and brick fragments.

4.1.1 Stratigraphic evidence of marine inundation

The detailaed stratigraphic sequence of the OSA-S6 core is described in Table 1, whereas Figure 4 shows the log of the OSA-S6 core (2.1 m long), considered representative for the Augusta Hospital site. Thus it will be discussed in the following with the aim of recognizing marine inundation deposits

Depth (cm)	Thickness interval	Description:
0-35	35 cm	Brown silty clay, with sparse macrofossils fragments, organic rich in its upper 25 cm (active soil horizon); the presence of brick pieces, particularly large (up to few cm) in its lowermost 10 cm may implies that this deposit could be interpreted either as a natural colluvium or as an artificial leveling of the site.
35-70	35 cm	Brown-greenish silty clay with calcarenite clasts (up to 1 cm large) and sparse small shell fragments.
70-80	10 cm	Dark brown fine silt with sparse roots and shell fragments (probably paleosol);
80-100	20 cm	Gray-greenish clayey fine sand (event AU-00) characterized by abundant marine benthic foraminifera, not always well preserved, rare entire gastropods (*Pirenella conica*, *Planorbis* sp.) and ostracods, important amount of shell fragments and vegetal remains; the micropaleontological analysis suggests a very shallow marine environment with a vegetated substrate
100-150	50 cm	Gray to pale brown clayey silt deposits of alluvial origin with rare reworked microfossils, some carbonatic clasts and few small potsherds.
150-160	10 cm	Dark gray-brownish organic silt with shell fragments and roots (probably a paleosol).
160-170	10 cm	Gravel layer (event AU-01) made by sub-angular carbonatic clasts (up to 3 cm) and by rare reworked forams, shell fragments and pottery within a dark gray brownish fine silt, rich in vegetal remains; it presents a sharp erosional, basal contact (Fig. 5a).
170-185	15 cm	Dark gray silt with sparse shell fragments; it originated in a brackish lagoonal environment marked by well preserved and abundant benthic lagoonal forams (*Ammonia tepida, A. parkinsoniana, Haynesina germanica,* Fig. 5b), rare shell fragments and gastropods (*P. conica* and *Hydrobia* spp); its base is rich in roots and seeds.
185-193	8 cm	Yellowish bioclastic layer (event AU-02, Fig. 5a) composed by few whole gastropods (*Hydrobia* spp., *P. conica*), abundant shell fragments (mollusks, corals and echinoderms), few ostracods, often broken benthic (*Ammonia* spp., *Bolivina* sp., *Cassidulina laevigata*, *Cibicides lobatulus*, *Haynesina germanica, Pullenia bulloides*, *Rosalina* spp., miliolids) and few badly preserved planktonic (*Globigerina* spp., *Globigerinoides* spp., *Globorotalia inflata*, *Turborotalita quinqueloba*) forams (Fig. 5c); sharp erosional basal contact and no evidence for layering or grading.
193-208	15 cm	Dark gray to gray fine silt with few sparse small pebbles and some roots; the micropaleontological analysis suggests a brackish lagoonal environment marked by well preserved benthic foraminifera (*A. tepida, A. parkinsoniana, H. germanica,* Fig. 5b), several whole gastropods (*Hydrobia* spp, *P. conica*) and abundant ostracods (mainly *Cyprideis torosa*).

Table 1 - Detailed description of the OSA-S6 core

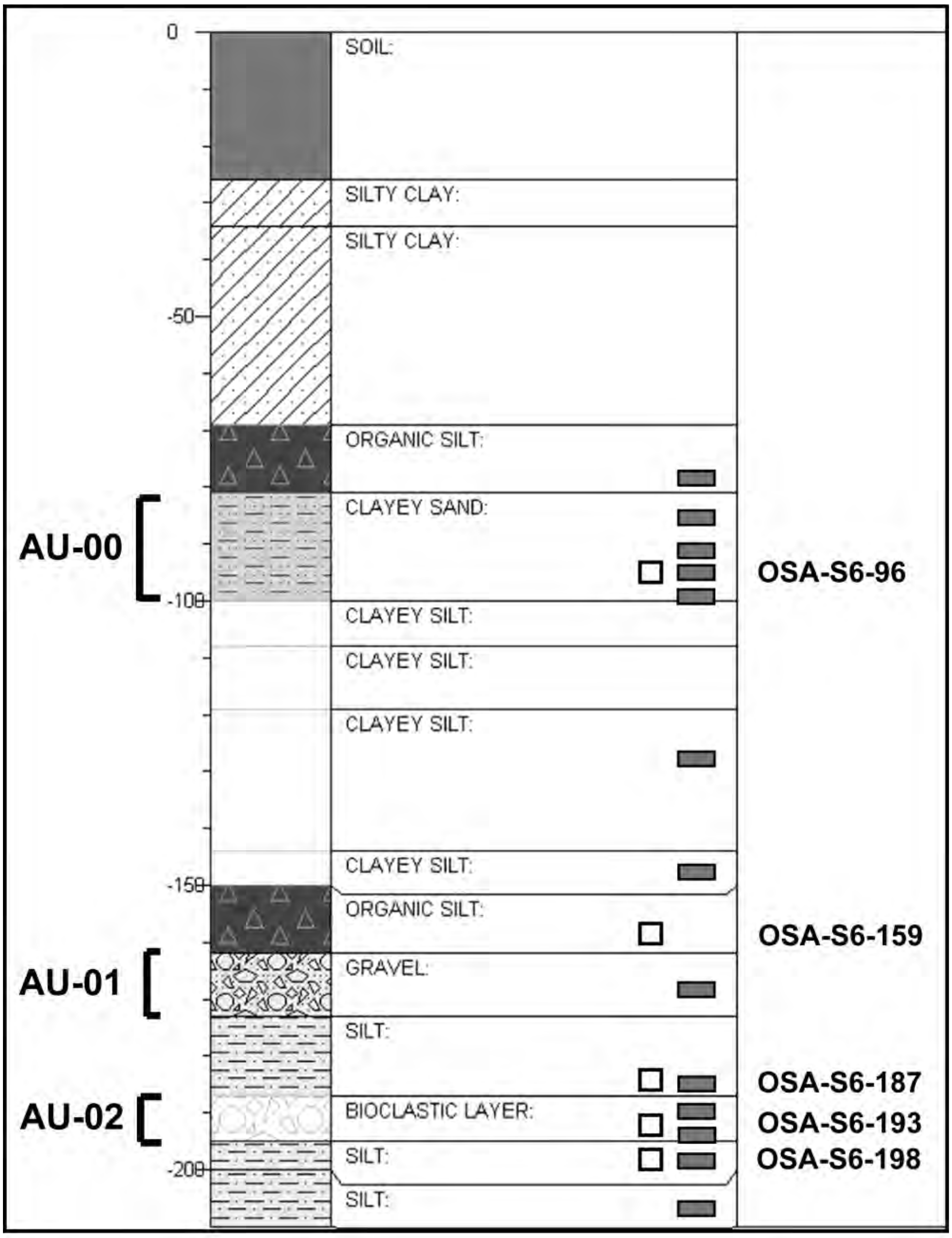

Fig. 4 – Core OSA-S6 log from the Augusta Hospital site; open squares locate C14 samples (with corresponding name on the right, see Table 1 for ages) while gray rectangles represent micropaleontological samples; on the left the stratigraphic position of the three marine inundations recognized is visualized by square brackets.

The OSA-S6 stratigraphy consists primarily of low-energy silty clay, clayey silt and silt deposits, contrasting with two “anomalous” coarse layers (the gravel and the bioclastic layers, event AU-01andevent AU-02 in Fig. 5). Both “anomalous” layers are made by about 10 cm thick sediments clearly coarser than above and below, are massive and structureless, characterized by sharp erosional lower contact and by significant shell detritus content. These layers represent high energy deposits of clear marine origin (planktonic and rare marine benthic foraminifera have been found) within a brackish lagoonal environment (Fig. 5). Furthermore, the younger one (AU-01) is also followed by a sudden change in depositional environment from brackish lagoon to slope alluvium, i.e. the transition (Fig. 4) from dark gray silt (below) to organic dark brown silt and pale brown clayey silt (above), probably related to a modification of the local morphological conditions.

Moreover, the micropaleontological analysis shows a sudden change from alluvial to marine environment at about 1.0 m depth (Fig. 4). On the basis of this change, we hypothesize also at this depth the occurrence of another event (the AU-00) possibly related to an earthquake/tsunami that induced a change in the morphology of the shoreline, or the disruption of the sand spit protecting this low-energy depositional area and the consequent abrupt environmental modification.

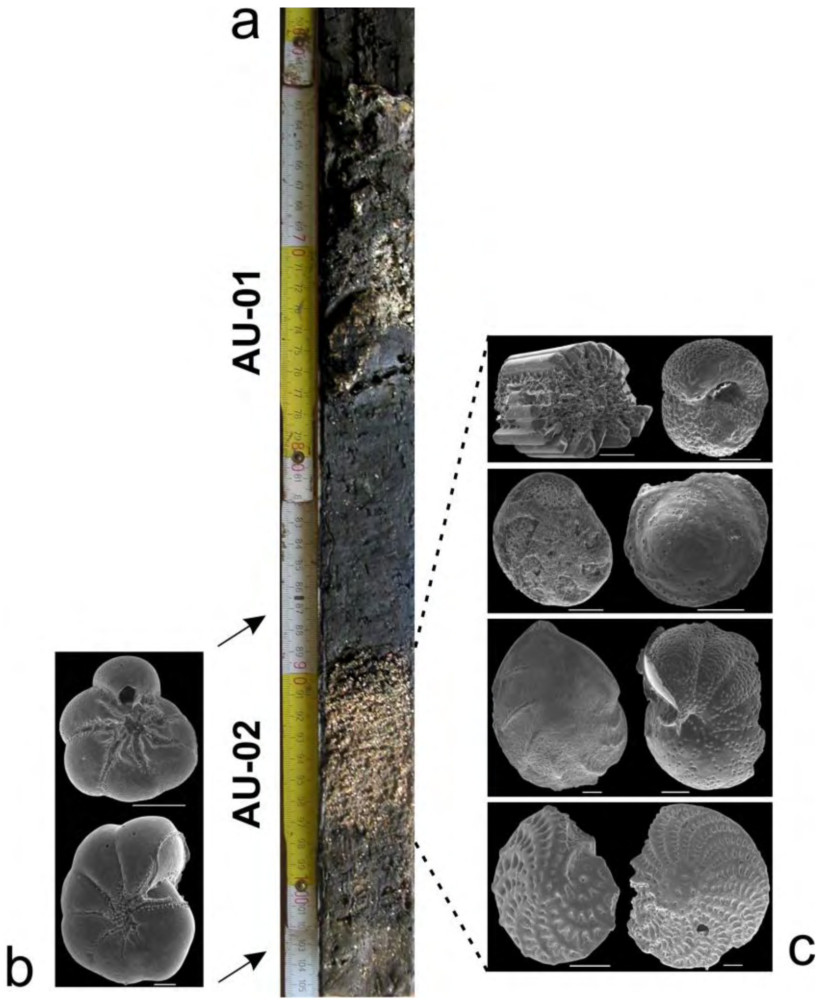

Fig. 5 – Augusta Hospital site: a) picture of the OSA-S06 core between 140 cm and 210 cm showing the bioclastic layer (AU-02 event) and the gravel layer with angular calcarenites clasts (AU-01 event); b) FESEM pictures (the scale bar represents 100 μm) of the benthic foraminifera assemblage typical of the lagoonal environment (from the top *Ammonia tepida* and *Haynesina germanica*) detected above and below the bioclastic layer; c) FESEM pictures (the scale bar represents 100 μm) of a coral fragment (photo on the uppermost left side), a planktonic foraminifera (*Globorotalia inflata* on the uppermost right side) and some selected benthic foraminifera species (clockwise starting from the

uppermost 2nd line *Rosalina bradyi, Asterigerinata mamilla, Lenticulina gibba, Cibicides lobatulus, Elphidium aculeatum, Elphidium crispum*) observed within the bioclastic layer.

4.1.2 Age constraints

Radiocarbon dating was performed on 5 samples from core OSA-S6 (Table 2, each sample is labeled with site code, core number and depth in cm).

The ages obtained are in stratigraphic order (no reversal) and suggest that the uppermost 2 m of the studied sequence are as old as about 3000 yrs.

Considering the depth of the dated samples with respect to the stratigraphic position of the marine inundations deposits, both AU-00 and AU-02 events ages are well confined by radiocarbon datings.

The abrupt environmental change (event AU-00) at about 1.0 m depth occurred very close to 650-770 AD, that is the age of OSA-S6-96 (Table 2 and Fig. 4), sampled just above it.

Event AU-01 is constrained between samples OSA-S6-187 and OSA-S6-159 yielding an age range of 900 BC-120 AD.

Finally, the age of event AU-02 can be constrained by the dating of the three samples OSA-S6-187, OSA-S6-193 and OSA-S6-198 that were collected just above, within, and below the bioclastic layer, respectively. These data constrain this marine inundation age to the interval 975-800 BC. The fact that the ages of these three samples are close in time, although collected at different depths, supports the hypothesis of a sudden inundation rather than a gradual transition to a higher energy environment.

Sample name/depth	Laboratory code	Type	Measured Age B.P.	δ^{13} C	Calibrated age 2 σ
OSA-S6-96cm	Poz-23118	Charcoal	1320± 30	-17.9	**650-770 AD**
OSA-S6-159cm	Poz-22862	Peat	1960± 30	-27.5	**40 BC -120 AD**
OSA-S6-187cm	Poz-20427	Peat	2685± 30	-22.8	**900-800 BC**
OSA-S6-193cm	Poz-20420	Bivalve *(Cerastoderma glaucum)*	3310± 30	-1.1	**1265-825 BC**
OSA-S6-198cm	Poz-20428	Peat	2745± 30	-16.5	**975-820 BC**
OPR-S11-44cm	Poz-20882	Bivalve *(Cerastoderma glaucum)*	890± 30	-2.6	**1420-1690 AD**
OPR-S11-66cm	Poz-22919	Gastropod *(Pirenella conica)*	2460± 35	-0.1	**225 BC-220 AD**
OPR-S1-158cm	Poz-20428	Bivalve *(Cerastoderma glaucum)*	3970± 35	0.7	**2100-1635 BC**

Table 2 - Measured and calibrated ages (according to Calib REV5.0.2 by Stuiver and Reimer, 2005) of the samples collected in the cores. For the marine shells we adopted the reservoir correction for marine samples (400 yrs according to the calibration data set marine04.14c, see Calib REV5.0.2 by Stuiver and Reimer, 2005) and a difference ΔR = 124±77 yrs in reservoir age of the study region, to accommodate local effects.

Although constant sedimentation rates could be considered inappropriate for a site where we have evidence for an environmental change from protected lagoon to coastal low-land, but they are similar all along the core, changing less than 10% if calculated for the whole core OSA-S6 or only for its uppermost 1 m (Tables 1, 2 and Fig. 4). We calculated average sedimentation rates of 0.7-0.5

mm/yr taking into account or excluding the 19 cm thickness of the marine inundation deposits and the possibly artificial uppermost 35 cm sediment, i.e. assuming erosion equal to high energy deposits thickness or null erosion, respectively. Thus, on the basis of the assumption of costant sedimentation rate we can narrow the age window of event AU-01 to about 600-400 BC. Finally, we have to mention that the lack of evidence for younger (historical) marine inundations may be due to erosional/depositional processes (both natural and artificial) affecting the uppermost 0.3-0.4 m of the Augusta Hospital site (see Fig. 4 and its description).

4.2 The Priolo Reserve site

The Priolo Reserve site (Fig. 2), located in the southern part of the bay about 10 km from the Augusta Hospital site, is a 0.5 km^2 shallow coastal lagoon separated from the sea by a thick bar of sand dunes, up to 4.5 m high (Fig. 6). Since Greek times (but well documented reports exist only since AD 1200) the northern part of the lagoon was used to produce marine salt, very important and precious for the tuna factory located nearby. Nowadays, this area is a Regional Natural Reserve (http://www.salinepriolo.it/) and has the optimal morphologic condition to represent a tsunami deposit trap.

In this site we performed 16 cores down to a maximum depth of 4.2 m, at a maximum distance from the coastline of 530 m. The core location followed a NNE-SSW trend from the central part to the edges of the lagoon.

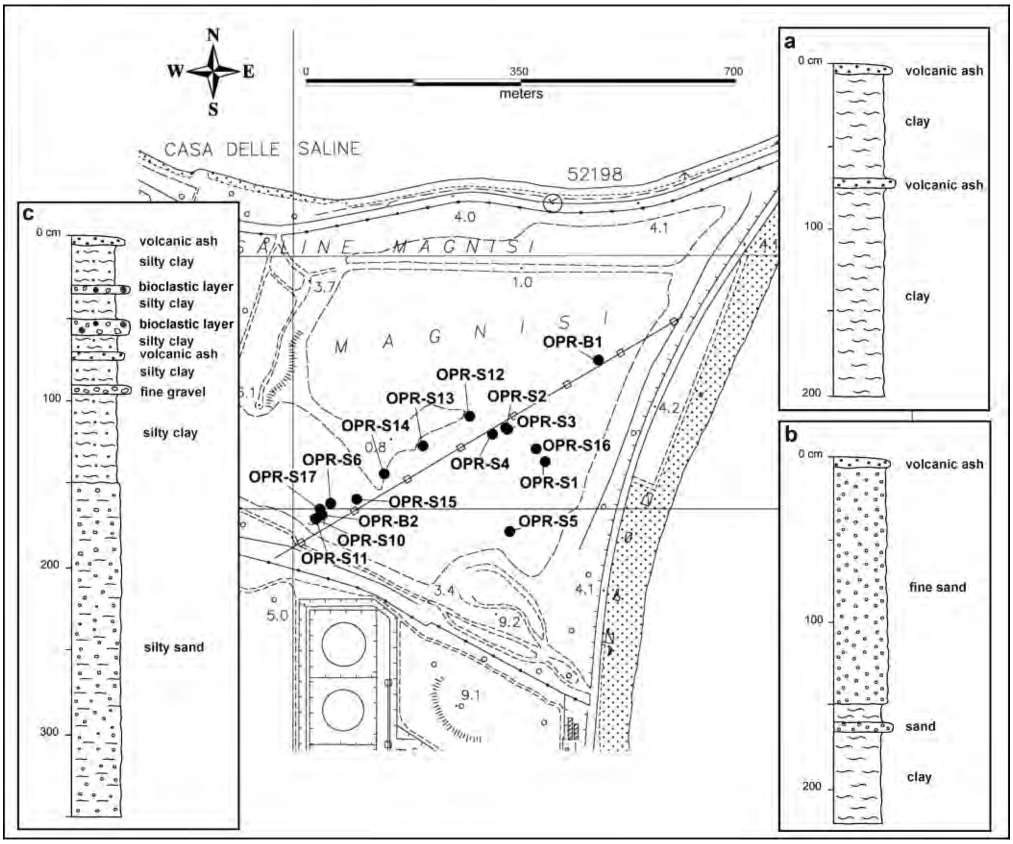

Fig. 6 – Detailed map of the Priolo Reserve site (based on RTC, 1:10000 scale); black dots represents cores location. a) b) and c) are the schematic stratigraphic logs of the sedimentary sequence found in the central, southeastern and southwestern part of the lagoon, respectively.

The stratigraphy revealed by these cores is not uniform and sedimentological changes are common from the central part of the lagoon southwestward and eastward, where the vicinity of sand dunes influence the local sedimentation (Fig. 6).

The cores in the central part of the lagoon (e.g. cores OPR-S2-S3-S4) contain about 2 m of light to dark gray clay with shell fragments, locally abundant, few entire gastropods and bivalves, vegetal remains, turning occasionally to clayey silt (log a in Fig. 6). The clay is interrupted by one peculiar dark brown to black few cm thick volcanic tephra layer (at about 0.7 m depth). At the surface a pellicular 1-3 cm thick layer of black fine volcanic ash made of small clasts of tachylite and sideromelane, is likely related to the 2002-03 Etna volcano eruption. In the south-eastern sector of the Reserve (e.g. core OPR-S1-S5), the cores show from about 2.2 to 1.5 m depth gray silty clay to clay layers with small shell fragments, interrupted by one distinctive, 2-4 cm thick, dark gray sand layer at about 1.6 m depth (log b in Fig. 6), followed by about 1.5 m thick brownish fine to medium well sorted sand (interpreted as sediments remobilized from the adjacent dunes) with shell fragments and few centimetric whole gastropods and lamellibranchs. Also in this area, at the surface, the thin volcanic ash layer was found.

The most interesting area for the research of marine inundation deposits was the southwestern sector of the lagoon (e.g. cores OPR-S6-S10-S11-S17). Here, from about 3.5 to 1.5 m depth the cores comprise yellowish sand to silty sand with sparse abundant carbonatic clasts, mm to cm in size. From 1.5 m depth to the surface the deposits (log c in Fig. 6) are dominated by gray to brown silty clay to clayey silt layers with shell fragments, vegetal remains and entire bivalves and gastropods. These fine deposits are interrupted by two distinctive 5 to 10 cm thick bioclastic layers at about 0.3 and 0.5 m depth, respectively, by one distinct dark brown to black 5 cm-thick volcanic ash at about 0.7 m depth and by one 2-3 cm thick detritic deposit at 0.9 m depth. Again at the surface we observed the thin volcanic ash layer, described above.

4.2.1 Stratigraphic evidence of marine inundation

The complete stratigraphic sequence of OPR-S11 core is shown in Table 3, whereas Figure 7 shows the upper 1.5 m log.

Depth (cm)	Thickness interval	Description:
0-30	30 cm	Pale brown silt to clayey silt deposit with vegetal remains and shell fragments (mainly mollusks); micropaleontological analysis suggests a lagoonal environment, characterized by benthic lagoonal foraminifera (*Ammonia tepida, A. parkinsoniana, Haynesina germanica*), abundant ostracods and some gastropods (*Hydrobia* spp., *Pirenella conica*).
30-35	5 cm	Bioclastic layer with sharp basal contact (PR-01), very rich in ostracods and gastropods (*Hydrobia* spp.) all arranged in a chaotic pattern, with several mollusks fragments and vegetal remains.
35-50	10-15 cm	Gray clayey silt with abundant shell fragments, whole bivalves (*Cerastoderma glaucum*) and gastropods (*P. conica*) and well preserved benthic lagoonal forams (mainly *A. tepida* and *A. parkinsoniana*).
50-60	10 cm	Bioclastic layer with sharp erosional basal contact (PR-02), with a huge amount of shell fragments, gastropods (*P.a conica*, with abrasions due to high energetic transport) and ostracods, benthic and few planktonic forams (with a peculiar increment in the benthic foraminifera specific diversity with respect to adjacent deposits); interestingly it may be subdivided in three smaller (2-3 cm thick) layers.
60-70	10 cm	Pale brown to gray silt with shell fragments and vegetal remains, sparse and scarce microfauna, consisting of benthic lagoonal forams (*A. tepida, A. parkinsoniana, H. germanica*), some ostracods and gastropods (e.g. *P. conica*).
70-74	3-4 cm	Dark brown to black normally graded volcanic layer with sharp basal contact (see following chapter for description of this tephra).
74-77	2-3 cm	Gray to light gray bioclastic layer, interpreted as a thanathocenosis related to the volcanic ash deposit above.
77-97	20 cm	Dark gray clayey silt with shell fragments (mainly mollusks) and vegetal remains, the microfauna appears dominated by benthic lagoonal forams as for deposits above.
97-142	45 cm	Dark brown silty clay with few sparse shell fragments, vegetal remains partially oxidized and few small (mm) clasts, the microfauna is very scarce.
142-152	10 cm	Pale gray to brownish sandy silt with several clasts (up to 1 cm), the microfauna is very scarce and the few foraminifera appear badly preserved.

Table 3 - Detailed description of the OPR-S11 core

The OPR-S11 core (3.4 m long) is considered representative for the southwestern sector of the Priolo Reserve site. Thus it will be discussed in the following with the aim of recognizing marine inundation deposits.

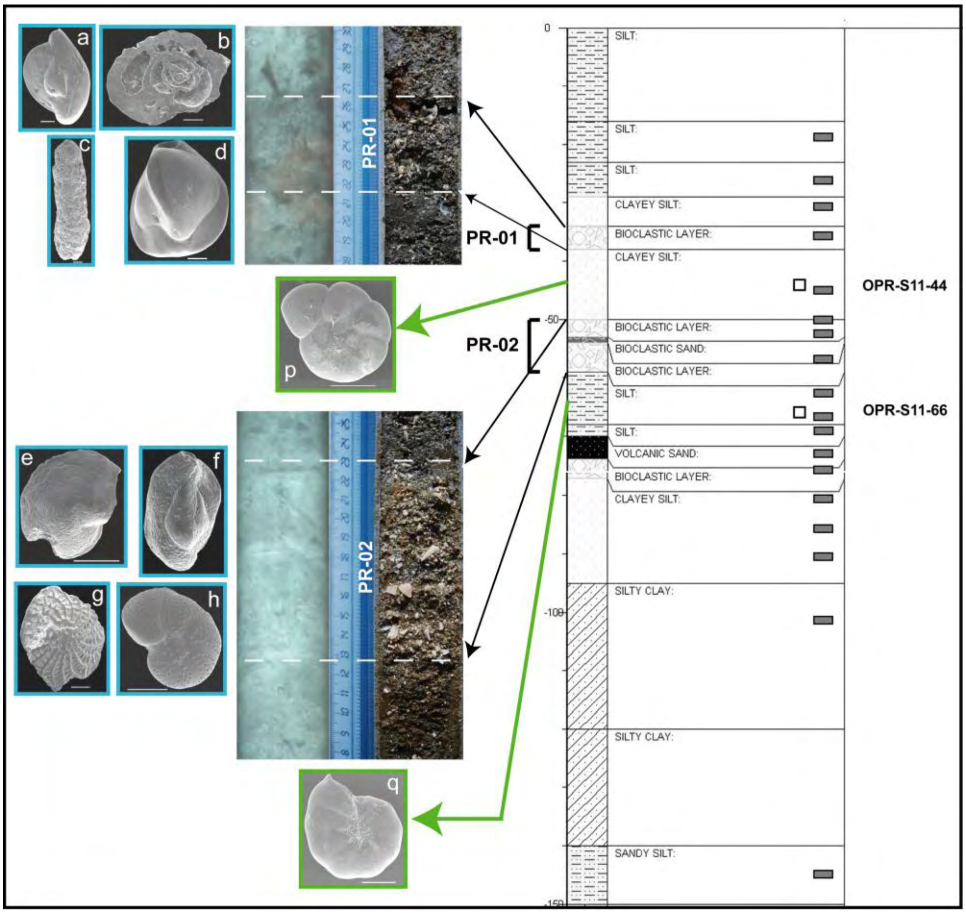

Fig. 7 – On the right: core OPR-S11 log (0-150 cm) from the Priolo Reserve site; open squares locate C14 samples (with corresponding name on the right, see Table 1 for ages) while gray rectangles represent micropaleontological samples; the stratigraphic position of the two marine inundations recognized is visualized by square brackets. On the left, above: picture and X-ray image of the uppermost bioclastic layer (event PR-01), a to d are FESEM pictures of marine foraminifera (*Adelosina* sp., *Nubecularia lucifuga*, *Bigenerina nodosaria* and *Triloculina* sp., respectively) found within this layer; below: picture and X-ray image of the lowermost bioclastic layer (event PR-02), e to h are FESEM pictures of marine foraminifera (*Cibicides lobatulus*, *Quinqueloculina* sp., *Elphidium crispum*, *Rosalina floridana*, , respectively) found within this layer;

finally p and q are FESEM pictures of lagoonal benthic foraminifera (*Ammonia* spp. and *Haynesina germanica*, respectively) found above and below the lowermost bioclastic layer (event PR-02). For all the FESEM pictures the scale bar represents 100 μm.

The stratigraphic and paleontological analyses of OPR-S11 core indicate that the whole sedimentary sequence belongs to a lagoonal low-energy environment. In fact, the fine deposits are all characterized by ostracods (*Cyprideis torosa*), bivalves and gastropods (*Hydrobia* spp.), specific of lagoonal environment, by lagoonal benthic foraminifera and few badly preserved marine foraminifera (likely reworked from inland older deposits). Exceptions are the two bioclastic deposits PR-01 and PR-02. These layers are composed by up to 10 cm thick sediments clearly coarser than above and below, showing absence of grading and characterized by sharp erosional lower contact (clearly visible on the XR film, see Fig. 7, as well as from the visual analysis). Moreover, both PR-01 and PR-02 deposits show an abnormal concentration of shell fragments and entire gastropods arranged in an unusual chaotic pattern. Interestingly, PR-02 layer also shows an internal subdivision that could be interpreted as the result of multiple waves.

These layers represent high energy deposits of clear marine origin (planktonic foraminifera and a peculiar increment in the benthic foraminiferal specific diversity have been found) within a lagoonal low-energy environment. In the Priolo Reserve site, further evidence for marine inundation deposits was derived from core OPR-S10 located near the core OPR-S11, where we found an unusual detritic deposit (PR-03) at about 0.9 m depth (Fig. 8 above). The analysis of core OPR-S10 highlighted that within a 100 cm thick sequence dominated by dark gray to gray clay with rare entire shells, macrofossil fragments, vegetal remains and scattered mm in size carbonatic clasts, apart from the volcanic tephra layer at about 0.7 m depth, there is a detritic deposit (PR-03, 2-3 cm thick) at about 0.9 m depth showing an anomalous assemblage made by macromammal bone fragments (Prof. A. Kotsakis, University of Roma Tre, personal communication), rare ostracods (*Cyprideis torosa*) and gastropods (*Hydrobia* spp.), together with badly preserved benthic (*Cassidulina carinata, Cibicidoides pseudoungerianus, Melonis barleanum, Planulina ariminensis*) and planktonic (*Globigerinoides* sp.) foraminifera, from shallow to deep marine environment.

Furthermore, a distinct sandy layer (PR-04, Fig. 8 below) has been detected at about 1.6 m depth (see Fig. 6 for core locations) in the southeastern sector of the lagoon in the OPR-S1 and OPR-S16 cores.

In the OPR-S1 core a peculiar dark gray fine sand layer (PR-04, 3 cm thick) with shell fragments was found within a 0.6-0.7 m thick deposit dominated by gray silty clay to clay with scarce and small shell fragments. Interestingly, in the PR-04 layer the marine microfauna, benthic (*Asterigerinata mammilla*, *Buccella granulata*, *Cibicides lobatulus*, *Elphidium* spp., *Nubecularia lucifuga*, *Quinqueloculina* spp., *Rosalina* spp.) and few planktonic (*Globigerinoides* spp.) foraminifera, as well as the marine macrofauna, appear well preserved, differently from the rare and poorly preserved paleontological association characterizing the fine to very fine deposits above and below it. Also in these cases the stratigraphic features of PR-03 and PR-04 imply rapid change from lagoonal, low-energy conditions to high-energy deposition of marine origin.

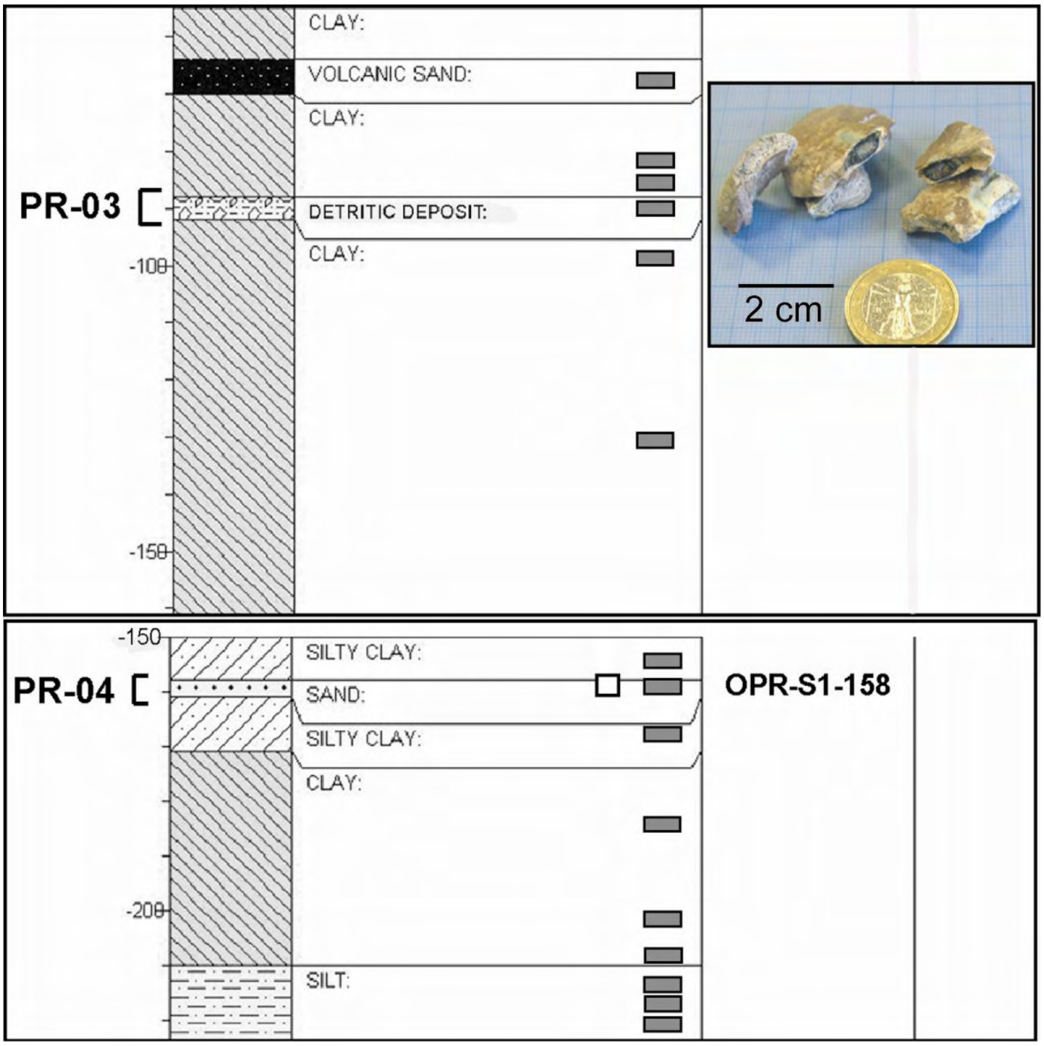

Fig. 8 – Above: OPR-S10 log (60-160 cm) from the Priolo Reserve site; gray rectangles represent micropaleontological samples; on the right picture of the macromammal bones fragments found within the detritic layer; the stratigraphic position of the marine inundation recognized is visualized by square brackets. Below: Core OPR-S1 log (150-220 cm) from the Priolo Reserve site; open square locates C14 sample while gray rectangles represent

micropaleontological samples; on the left the stratigraphic position of the marine inundation recognized is visualized by square brackets.

4.2.2 Age constraints

By integrating tephra and radiocarbon chronologies we established the age of the high-energy deposits found in the Priolo Reserve site. The ages obtained are in stratigraphic order (no reversal) and suggest that the uppermost 1.6 m of the studied sequence is as old as about 4000 yrs.

Teprochronology

In the Priolo Reserve site a 3-4 cm-thick black lapilli and ash layer was found in 6 cores at about 0.7 m depth. This layer is normally graded from cm-lapilli to coarse ash showing a sharp contact at the base. This deposit is homogenously dispersed in the investigated area as indicated by nearly constant thickness observed in the cores. This feature is typical of fallout deposition process according to which the deposit tends to blanket the original topography (Cas and Wright, 1987).

On the basis of morphoscophic analyses by optical microscope, the deposit results composed of well vesiculated scoriaceous clasts (sideromelane and tachylite), loose crystals of plagioclase and minor olivine and lava lithics, occasionally oxided.

Glass compositions in the sideromelane clasts were measured with a LEO-1430 scanning electron microscope equipped with an Oxford EDS micro-analytical system (SEM-EDS) at INGV Sezione di Catania laboratories (Table 4). Analytical conditions were 20 keV of acceleration tension, 1200 nA of beam current and XPP data reduction routine. To minimize alkali loss during analysis, a square raster of 10 micron was used. Replicate analyses of the international standard VG-2 glass basaltic (Jarosewich et al. 1980) were performed as analytical control. The precision expressed as relative standard deviation was better than 1% for SiO2, Al2O3, FeOtot and CaO and better than 3% for TiO2, MnO, Na2O, K2O and P2O5.

Samples show alkaline affinity and mugearitic composition, falling within the trend of Etna volcanics, in the total alkali versus silica diagram (TAS; Le Bas et al., 1986; Fig. 9). Petro-chemical and stratigraphic characteristics allowed us to correlate this tephra layer with the fallout deposit produced by the 122 BC plinian Etna eruption (Coltelli et al., 1998).

Sample	OPR S6-9	OPR S6-9	OPR S6-9	OPR S10-5	OPR S10-5	OPR S10-5	122 BC	122 BC	122 BC
SiO2	51.35	50.66	51.21	51.14	50.79	50.56	52.83	51.68	52.88
TiO_2	1.85	1.85	1.86	1.76	1.81	1.85	1.88	1.88	1.82
Al_2O3	16.65	16.48	17.03	17.15	16.76	16.72	17.13	16.82	16.76
$Fe_2O_3{}^T$	9.33	9.28	8.64	8.98	9.43	9.37	8.95	8.95	9.35
MnO	3.15	3.31	3.15	0.19	0.17	0.18	0.23	0.19	0.14
MgO	3.15	3.31	3.15	3.20	3.28	3.26	3.21	3.27	3.27
CaO	7.49	7.44	7.43	7.57	7.48	7.56	7.09	6.84	6.87
Na_2O	4.00	4.24	4.33	4.55	4.33	4.59	4.02	4.21	4.13
K_2O	2.52	2.46	2.30	2.35	2.45	2.46	3.10	3.24	2.89
P_2O_5	0.71	0.72	0.72	0.68	0.70	0.67	0.83	0.70	0.74
Total	97.80	97.14	97.36	97.57	97.18	97.23	99.26	97.77	98.86

Table 4 - Electron microscope (SEM-EDS) analyses of representative glass (major elements in wt%) in the Priolo tephra samples compared with 122 BC plinian Etna eruption composition.

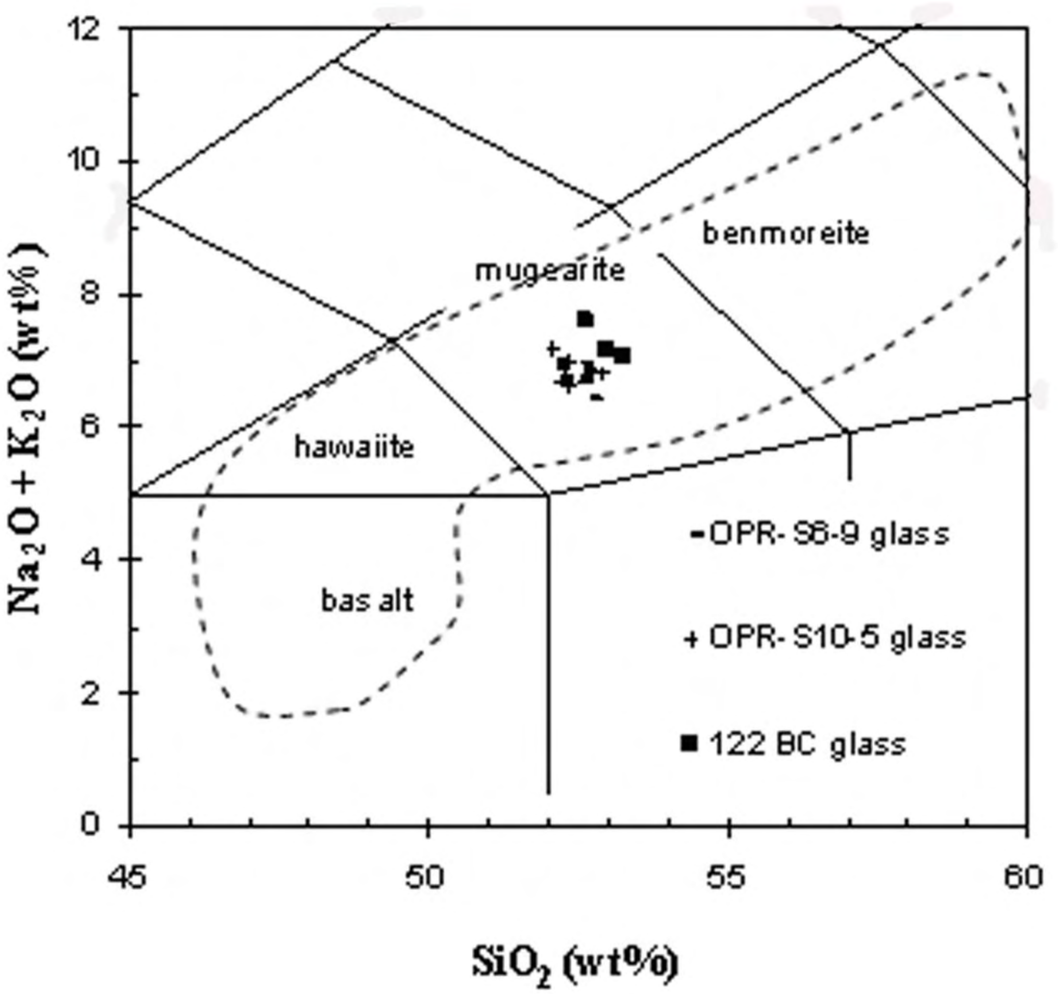

Fig. 9 – Total Alkali Silica classification diagram (TAS; Le Bas et al., 1986) showing glass compositions of tephra recovered in Priolo Reserve site (OPR-S6 and OPR-S10 cores) and from the 122 BC plinian eruption of Etna (Coltelli et al., 1998). Dashed line includes the composition of Mt Etna volcanics (Corsaro and Pompilio, 2004).

The 122 BC eruption is the largest explosive event of Etna volcano occurred in the Holocene and represents a major marker horizon in the stratigraphy because of its broad dispersal. The eruption caused copious lapilli and ash

fallout in the SE Etna volcano flank as also reported by Roman chronicles that described severe damage to the ancient town of Catania and surroundings. The 122 BC tephra was found at several localities up to 400 km far from the volcano summit in the Ionian Sea (Coltelli et al., 1998). The Priolo Reserve site is located along the main dispersal fallout direction and the thickness of the deposit is coherent with the decreasing thickness trend with distance from the vent of a pyroclastic fall deposit. In addition, the glass composition of Priolo Reserve samples is analogous to those of 122 BC juvenile clasts (Fig. 9).
This similarity along with the componentry of the deposit and its volcanological characteristics indicate that the Priolo Reserve tephra layer belongs to the 122 BC eruption of Etna.

Radiocarbon

Radiocarbon dating was performed on 3 shell specimens (Table 2), 2 from core OPR-S11 and 1 from core OPR-S1. Taking into account the depth of the dated samples with respect to the stratigraphic position of the marine inundation deposits, we may assert that PR-01 and PR-04 events ages are well constrained by radiocarbon datings.
Event PR-01 (Fig. 7) should be slightly younger than 1420-1690 AD that is the age of OPR-S11-44 (Table 2 and Fig. 7), sampled just below it. .
Event PR-02 is constrained between the tephra and the sample OPR-S11-44 that translates into the interval 122 BC-1690 AD.

The age of the event PR-03 (Fig. 8), found at 0.9 m depth in core OPR-S10 is older than 122 BC (age of the tephra found at 0.64-0.70 m depth). Finally, the age of event PR-04 is defined by sample OPR-S1-158 that was collected within the “anomalous” sand layer and thus its age (2100-1635 BC) should be considered as the PR-04 event age. Combining radiocarbon with tephrochronostratigraphic data, we obtain an average sedimentation rate for OPR-S11 core of 0.35-0.25 mm/yr. These values are calculated taking into account or excluding the 13 cm thickness of the proposed marine inundation deposits, i.e. assuming erosion equal to high energy deposits thickness or null erosion, respectively. Assuming this sedimentation rate, the age interval of the event PR-02 can be narrowed to 160-320 AD.

In a similar way, using the 0.33 mm/yr sedimentation rate derived by the volcanic ash found in core OPR-S10, the age of event PR-03 should be around 800-600 BC. To reduce the time interval of PR-02 and of PR-03 events we had to assume a constant sedimentation rate. Differently from the Augusta Hospital site, in the Priolo Reserve area this assumption appears very trustable, considering that tephrochronostratigraphic and C14 data provide a strictly comparable sedimentation rate, together with the absence of obvious erosional phases in the stratigraphic sections studied within the lagoon.

5. Discussion

The multi-theme approach based on historical studies, geomorphic-geologic surveys and laboratory analyses on the cores sediments allowed us to detect several high-energy deposits of marine origin in low-energy depositional environments. In the following we discuss the evidence supporting or against their tsunami origin.

The geological data collected at the Augusta Hospital and Priolo Reserve sites provide evidence for an exceptional record of six to seven marine inundations (tsunamis or storms) occurred during the past 4 ka. Then, since only a combination of different data can allow to discriminate between storm- or tsunami-derived deposits (Kortekaas and Dawson, 2007; Morton et al., 2007), in the following we discuss sedimentological and paleontological characteristics of the studied layers, their distance from the shoreline, their ages and frequency with respect to available catalogues and previous studies, to define the most likely process of emplacement.

At the Augusta Hospital site, we found evidence for three marine inundations (AU-00, AU-01 and AU-02 events, see Figs 4 and 5).

We suggest that the AU-01 and AU-02 characteristics are consistent with a tsunami inundation (*sensu* Morton et al., 2007). In fact, both AU-01 and AU-02 layers have been identified as relatively thin (about 10 cm) single massive and structureless beds with abrupt erosional lower contact. All these physical attributes tend to favor a tsunami origin. Moreover, the third event (AU-00) is characterized by a sudden change in depositional environment, from alluvial to marine, and the related layer (clayey fine sand about 20 cm thick) displays an important amount of shell fragments and vegetal remains but it lacks a clear differentiation in terms of grain size (from clayey silt to clayey fine sand). We decided to interpret the latter deposit as due to a tsunami wave but we cannot rule out the hypothesis that a local earthquake produced a significant coseismic modification of the coastline, disrupting the morphologic barrier able to protect the site area.

At the Priolo Reserve site, we found evidence for four marine inundations (PR-01 to PR-04 events, see Figs 7 and 8).

We suggest that the PR-01 and PR-02 physical attributes are consistent with a tsunami inundation (*sensu* Morton et al., 2007). In fact, both PR-01 and PR-02 bioclastic layers consist of relatively thin (about 10 cm) single massive and chaotic beds, with increment in the benthic foraminifera specific diversity and abrupt erosional lower contact. Also in these cases, these physical attributes tend to favor a tsunami origin. Furthermore, the third anomalous deposit, PR-03, is a thin (about 3 cm) single massive and structureless detritic layer showing an anomalous assemblage made by macromammal bone fragments, ostracods and gastropods, badly preserved benthic and planktonic foraminifera (from both shallow and open marine environment). The peculiar presence of macromammal bone fragments together with the coarser grain size of this deposit, with respect to the clay layers dominating the local sequence, suggest us to interpret the PR-03 detritic layer as the deposit of a tsunami back-wash wave, possibly capable to transport and deposit such heterogeneous layer.

Finally the forth deposit, PR-04, is made by a thin (about 3 cm) single massive fine sand bed, clearly coarser and characterized by a very different paleontological association with respect to the very fine deposits above and below it. Sedimentological, morphological and paleontological characteristics of PR-04 deposit may well be interpreted as the result of an important tsunami wave.

As discussed above, another key element to distinguish tsunami or storm deposits is the distance of the anomalous layers with respect to the shoreline. To estimate the maximum inundation distance of extreme meteorological events (storms) of the Mediterranean Sea at the study sites, we analysed the anemometric and ondametric data (see also Barbano et al., 2010), recorded by the meteo-marine Catania station (located about 35 km north of the study area) belonging to the RON - Rete Ondametrica Nazionale (= Italian Ondametric Buoy Network, www.idromare.it) for the available period 1989–2006 and we calculated the maximum water flooding of these events at the investigated sites (Table 5). The results suggest that the strongest recorded storms have an inundation distance confined within 55 m from the coast.

Table 5. Storm events with maximum wave height (H_0) and peak period (T_0) in deep water recorded by Catania buoy, and H_b and X_{max} for Augusta and Priolo sites (modified from Barbano et al., 2010).

Date	Wave data from Catania buoy			Wave data in Augusta site				Wave data in Priolo site			
	Direction (N)	H_S	T_P	L_0 (m)	β_1(°)	AWH_b (m)	AX_{max} (m)	L_0 (m)	β_2(°)	PWH_b (m)	PX_{max} (m)
31/03/1991	70°	5.1	9.1	129.3	0.6	4.6	12	147.6	0.7	4.7	13
26/12/1992	94°	5.8	11.1	192.4		5.6	16	204.8		5.7	18
28/02/1996	104°	6.2	11.1	192.4		5.9	18	201.6		6.1	19
17/03/2003	162°	3.8	13.3	276.3		4.5	22	404.4		4.6	22
04/10/2004	40°	4.1	28.6	1277.7		6.9	52	1546.1		7.1	53
05/01/2005	129°	3.0	28.6	1277.7		5.5	40	1454.1		5.7	45
12/01/2005	119°	3.3	28.6	1277.7		5.9	41	1383.5		6.1	47

β_1 and β_2 are the average sea bottom slope from −20 m depth to the shoreline at Augusta and Priolo respectively, as measured from the nautical maps of the Italian Marine Hydrographic Institute (Istituto Idrografico della Marina, 1999) at scale 1:100.000. The estimated wave length in deep water ($L_0=gT^2/2\pi$; Sarpkaya and Isaacson, 1981) and the wave height at breaking point at

Augusta (AWH_b) and Priolo (SWH_b), are determined with the Sunamura and Horikawa (1974) equation ($Hb/H0=(\tan\beta)^{0.2}(H0/L0)^{-0.25}$). AX_{max} = Augusta; PX_{max} = Priolo are the maximum water flooding of the strongest storm waves in the study areas, obtained using the equations of Cox and Machemel (1986) and Noormets (2004).

Furthermore, at both Augusta Hospital and Priolo Reserve sites the evidence for the marine inundations was collected at about 400-500 m from the present shoreline, a tsunami origin for the deposits investigated should be preferred. Another consideration may strengthen the tsunami origin of the older events that occurred when, according to Lambeck et al. (2004) and Antonioli et al. (2009), the sea level was possibly few meters lower than the present. Following this interpretation, for the events older than about 2000 years, we may consider to add an extra distance of the sites with respect to the shoreline at that time, taking into consideration that the isobaths -5 m is located ca. 600 m offshore. Obviously, this would make the case for really huge inundations!

Another information that may help in the discrimination between storm and tsunami origin is the frequency of these extreme events, knowing that, compared to coastal storms, major tsunamis are less frequent events (Morton et al., 2007). According to the ERA-40 dataset for the Ionian Sea (a re-analysis of global atmosphere and surface conditions from September 1957 through August 2002 – by Spirito, 2006) nine strong cyclones occurred during the 45 years. With this frequency we would expect ca. 800 exceptional storms during the 4000 yrs long time interval recorded in the cores, an amount of two orders of magnitude larger than the number of marine inundations detected in the Augusta bay.

Finally, also the age ranges established for some of the inundation events are supporting the hypothesis of tsunami as cause.In fact, the four inundation events found at the Priolo Reserve site were dated at: PR-01 slightly younger than 1420-1690 AD; PR-02 160-320 AD; PR-03 800-600 BC and PR-04 2100-1635 BC, and three of them can be associated to historical tsunamis occurred in the Ionian Sea and further east. PR-01 deposit can be related to the 1693 tsunami; PR-02 can be linked to the 365 AD Crete tsunami and PR-04 could be tentatively associated to the ~3600 BP Santorini event (Friedrich et al., 2006). No age correlation can be made in the Augusta Hospital site because the age of the detected marine inundations (AU-00 650-770 AD; AU-01 600-400 BC; AU-02 975-800 BC) is too old and the relative historical record very scarce.
About the 1693 tsunami, geological evidence for the transport of big boulders related to this event has been recently suggested (Scicchitano et al., 2007) for two sites, namely the Magnisi Peninsula (in front of the Priolo Reserve site about 1 km to the east, Fig. 2) and the Maddalena Peninsula (about 15 km to the south in the Siracusa Bay, Fig.1a); thus, our data are in agreement and corroborate these previous findings. As regards the 365 AD Crete tsunami, its deposit has never been found so far in certain sedimentary evidence (see Scheffers and Scheffers, 2007 for a review) and so we do not have an original deposit and/or a site to compare with. Our association of the PR-02 deposit to the 365 AD Crete tsunami is in agreement with historical data (Jerome, 380) and tsunami wave modeling works (Lorito et al., 2008; Shaw et al., 2008) but investigation of other sites along eastern Sicily and elsewhere in the Mediterranean Sea together with more datings are needed to better understand

this event that destroyed many cities and drowned thousands of people in coastal areas from Egypt to Croatia (Guidoboni et al., 1994; Stiros, 2001). Finally, about the possibility to associate event PR-04 to the Late Minoan Santorini event, limited onshore field evidence has been found so far in the Mediterranean region (Dominey-Howes, 2004) apart from the Santorini island (McCoy and Heiken, 2000). Possible findings of the Santorini tsunami deposits are from Greece (Bruins et al., 2008) in sites located along the northern shore of the Crete island (about 150 km far), from south-western Turkey (Minoura et al., 2000) in the Didim and Fethye sites (about 200 and 350 km far, respectively) and from Israel (Goodman-Tchernov et al., 2009) in the continental shelf off Israel (about 1000 km far). These deposits, distributed only to the NE-E-SE with respect to the tsunami source, are quite different and a comparison with our findings is not feasible. The distance of our sites from the Santorini island (about 900 km westward) is comparable with those of published papers and thus it may represent the first onshore evidence in the central-western Mediterranean area. In fact, the westernmost evidence (about 600 km far) comes from deep-sea homogenite deposits attributed to a possible Late Minoan Santorini tsunami (Cita and Aloisi, 2000 and references therein).

6. Conclusions

On the basis of the combination of all the data collected on the marine inundations that hit the Augusta Bay area, we suggest that evidence for at least six tsunami events was found at the Augusta Hospital and Priolo Reserve sites during the past 4 ka. In terms of tsunamis timing, we could list them as follow:

younger than 1420-1690 AD (PR-01), 650-770 AD (AU-00), 160-320 AD (PR-02), 600-400 BC (AU-01), 800-600 BC (PR-03), 975-800 BC (AU-02) and 2100-1635 BC (PR-04). A question that remains open, because of the possible overlap of their ages, regards the possibility of associating PR-03 and AU-01 or AU-02 deposit to the same tsunami event.

Three of the tsunami deposits found at the Priolo Reserve site may be associated to historical tsunamis: PR-01 to the 1693 local event, PR-02 to the 365 AD Crete event and PR-04 to the ca. 3600 BP Santorini event. These results appear to confirm previous studies developed in the same area on the 1693 tsunami. For the 365 AD Crete tsunami and the Late Minoan Santorini event, our findings may represent the first onshore evidence in the central-western Mediterranean area. On the basis of these results we can assume a geologic ATRI of about 600 years for the past 4 ka in the Augusta Bay. If we compare this result with the historical ATRI of about 250 years, we may note that we missed some events. There are two main reasons for this discrepancy: a) the historical reports for the last millennium recorded tsunamis that possibly were not so strong in the Augusta Bay area to carry deposit and preserve sediments a few hundred meters inland (e.g. the 1908 run-up is about 2 m and its inundation apparently did not penetrate inland more than 20 m, Fig. 1c), b) the inland tsunami research suffers the difficulties related to the intense human activity along the coastline and superficial erosional processes that may remove tsunami signatures, especially in recent times (the Augusta Hospital site may be a good example). As a consequence, we should consider the opportunity to make an important effort in the offshore tsunami research, where the evidence for such exceptional events may be better preserved (Abrantes et al., 2008; Dawson and Stewart, 2008; Goodman-Tchernov et al., 2009).

We should mention that the research of tsunami deposits in eastern Sicily is a new line of research only recently undertaken (Scicchitano et al., 2007; Pantosti et al., 2008; Barbano et al., 2010) and thus the different approaches used for the identification and dating of tsunami deposits need further testing, systematization and formalization.

In conclusion, we believe that the identification and characterization of tsunami deposits in the same area may provide a unique opportunity to obtain realistic average tsunami recurrence interval, minimum inundation distance, elapsed time since the last tsunami event. This information is extremely relevant for testing and constraining tsunami scenario and modeling for Civil Protection applications.

5. Acknowledgements

This work was funded by the Italian Dipartimento della Protezione Civile in the frame of the 2004-2006 and 2007-2009 agreements with Istituto Nazionale di Geofisica e Geofisica e Vulcanologia – INGV with contribution of the EU Transfer project. We are indebted with Dott. L. Gasperini, from ISMAR-CNR-Geologia Marina, Bologna, for the help provided for the susceptibility and X-ray analyses. Many thanks also to E. Lipparini and G. Marozzi for the technical support kindly offered in the ISMAR-CNR labs. Prof. E. Gliozzi from Roma Tre University is thanked for assistance with ostracodes and mollusks analyses. L.

Miraglia is kindly acknowledged for assistance of SEM-EDS analyses performed at Istituto Nazionale di Geofisica e Vulcanologia, Sezione di Catania. PDC is grateful to G. Saviozzi for making thin sections of tephra samples.
We wish to thank Prof. G. Mastronuzzi and an anonymous reviewer whose suggestions contributed to improve the original manuscript.

6. References

Abrantes, F., Alt-Epping, U., Lebreiro, S., Voelker, A., Schneider, R., 2008. Sedimentological record of tsunamis on shallow-shelf areas: The case of the 1969 AD and 1755 AD tsunamis on the Portuguese Shelf off Lisbon. Marine Geology, 249 (3-4), 283-293.
AgdS, 1693. Archivio General de Simancas, Secretaría de Estado, Negociación de Sicilia, legajo 3507 (1693-1694). Consultas decretos y notas, n. 11, Relazione dei luoghi che hanno sofferto in Sicilia nei Terremoti dal nove di gennaio fino al cinque di febbraio del 1693 che si sono sentite ventuno scosse, le prime tre grandi e le altre più lievi, Palermo.
Antonioli, F., Ferranti L., Fontana A., Amorosi A., Bondesan A., Braitenberg C., Dutton A., Fontolan G., Furlani S., Lambeck K., Mastronuzzi G., Monaco C., Spada G., Stocchi P., 2009. Holocene relative sea-level changes and vertical movements along the Italian and Istrian coastlines. Quaternary International, 206, 102-133.
ASV, 1693. Archivio Segreto Vaticano, Segreteria di Stato, Inquisizione Malta, vol. 44, cc. 11-16, Relazione dell'Inquisitore di Malta F. d'Acquaviva al

Segretario di Stato Cardinale Spada sui danni causati a Malta e in Sicilia dal terremoto dell'11 gennaio 1693, Malta 18 gennaio 1693.

Atwater, B.F., Hemphill-Haley, E., 1996. Preliminary estimates of tsunami recurrence intervals for great earthquakes of the past 3500 years at Northeastern Willapa Bay, Washington. U.S. Geological Survey Open-File Report, 96-001.

Atwater, B.F., Moore, A.L., 1992. A tsunami about 1000 years ago in Puget Sound, Washington. Science, 258, 1614-1617.

Baratta, M., 1910. La catastrofe sismica calabro-messinese (28 Dicembre 1908). Relazione alla Società Geografica Italiana, 426 pp. Roma.

Barbano M.S., Pirrotta C., Gerardi F., 2010. Large boulders along the south-eastern Ionian coast of Sicily: storm or tsunami deposits? Submitted to Marine Geology.

Barbano, M.S., Rigano, R., 2001. Earthquake Sources and Seismic Hazard in South-eastern Sicily. Annali di Geofisica, 44 (4), 723-738.

Boccone, P., 1697. Intorno il terremoto della Sicilia seguito l'anno 1693. Museo di Fisica, Venezia.

Bottone, D., 1718. De immani Trinacriae terraemotu. Idea historico-physica, in qua non solum telluris concussiones transactae recensentur, sed novissimae anni 1717. Messina.

Boschi, E., Guidoboni, E., Ferrari, G., Gasperini, P., Mariotti, D., Valensise, G., 2000. Catalogue of strong earthquakes in Italy from 461 B.C. to 1997. Annali di Geofisica, 43 (4), 843-868 and CD-ROM.

Bruins, H.J., MacGillivray J.A., Synolakis, C.E., Benjamini, C., Keller, J., Kisch H.J., Klügel, A., van der Plicht, J., 2008. Geoarchaeological tsunami deposits at Palaikastro (Crete) and the Late Minoan IA eruption of Santorini. Journal of Archaeological Science 35, 191-212.

Burgos, A., 1693. Distinta relazione avuta per lettera del P. Alessandro Burgos scritta ad un suo amico, che contiene le notizie fin'ora avute de' danni cagionati in Sicilia da terremoti a 9 e 11 gennaio 1693. Palermo-Roma.

Campis, P.,1694. Disegno historico o siano l'abbozzate historiae della nobile e fidelissima città di Lipari (ms. 1694), in: Iacolino, G. (Ed.), Lipari, 1991.

Cas R.A.F., Wright J.W., 1987. Volcanic successions. Chapman and Hall Editors, 528 pp.

Cita, M.B., Aloisi, G., 2000. Deep sea tsunami deposits triggered by the explosion of Santorini (3500 y BP), eastern Mediterranean. Sedimentary Geology 135, 181–203.

Clague, J. J., Bobrowsky, P. T., Hamilton, T. S., 1994. A sand sheet deposited by the 1964 Alaska tsunami at Port Alberni, British Columbia. Estuarine, Coastal and Shelf Science, 38 (4), 413–421.

Cochran, U. A., Berryman, K., Mildenhall, D., Hayward, B., Southall, K., Hollis, C., 2005. Towards a record of Holocene tsunami and storms for northern Hawke's Bay, New Zealand. New Zealand Journal of Geology and Geophysics, 48, 507–515.

Coltelli, M., Del Carlo, P., Vezzoli, L., 1998. The discovery of a Plinian basaltic eruption of Roman age at Etna volcano (Italy). Geology, 26, 1095-1098.

Corsaro, R. A., Pompilio, M., 2004. Dynamics of magmas at Mount Etna, in: Bonaccorso, A., Calvari, S., Coltelli, M., Del Negro, C., Falsaperla, S. (Eds.), Mt. Etna: Volcano Laboratory; AGU Geophysical Monograph Series 143, pp. 91-110.

Cox, J.C., Machemehl, J., 1986. Overland bore propagation due to overtopping wave. Journal of Waterway, Port, Coastal and Ocean Engineering, 112, 161–163.

CPTI Working group, 2004. Catalogo Parametrico dei Terremoti Italiani, version 2004 (CPTI04). INGV, Bologna. http://emidius.mi.ingv.it/CPTI/.

De Martini, P.M., Burrato, P., Pantosti, D., Maramai, A., Graziani, L., Abramson, H., 2003. Identification of liquefaction features and tsunami deposits in the Gargano area (Italy): a geologic contribution to the hazard assessment. Annals of Geophysics, 46 (5), 883-902.

Dawson, A.G., Stewart, I., 2008. Offshore tractive current deposition: the forgotten tsunami sedimentation process. In: Shiki, T., Tsuji, Y., Yamazaki, T., Minoura, K., (Eds.), Tsunamiites - Features and Implications, pp. 153-161. Elsevier, Amsterdam.

Dawson, A.G., Stewart, I., 2007. Tsunami deposits in the geological record. Sedimentary Geology, 200 (3–4), 166–183.

Dawson, A.G., Hindson, R., Andrade, C., Freitas, C., Parish, R., Bateman, M., 1995. Tsunami sedimentation associated with the Lisbon earthquake of 1 November AD1755: Boca de Rio, Algarve, Portugal. The Holocene, 5 (2), 209-215.

Dominey-Howes, D.T.M., 2004. A re-analysis of the Late Bronze Age eruption and tsunami of Santorini, Greece, and the implications for the volcano-tsunami hazard. Journal of Volcanology and Geothermal Research, 130, 107-132.

Dominey-Howes, D.T.M., Humphreys, G.S., Hesse, P.P., 2006. Tsunami and paleotsunami depositional signatures and their potential value in understanding the late-Holocene tsunami record. The Holocene, 16, 1095–1107.

Fazello, T., 1560. De rebus Siculis decades duae. Palermo.

Friedrich, W.L., Kromer, B., Friedrich, M., Heinemeier, J., Pfeiffer, T., Talamo, S., 2006. Santorini eruption radiocarbon dated to 1627e1600 B.C. Science, 312, 548.

Fujiwara, O., 2008. Bedforms and sedimentary structures characterizing tsunami deposits. In: Shiki, T., Tsuji, Y., Yamazaki, T., Minoura, K., (Eds.), Tsunamiites - Features and Implications, pp. 51-62. Elsevier, Amsterdam.

Fujiwara, O., T. Kamataki, 2008. Tsunami depositional processes reflecting the waveform in a small bay: interpretation from the grain-size distribution and sedimentary structures. In: Shiki, T., Tsuji, Y., Yamazaki, T., Minoura, K., (Eds.), Tsunamiites - Features and Implications, pp. 133-152. Elsevier, Amsterdam.

Gelfenbaum, G., Jaffe, B., 2003. Erosion and sedimentation from the 17 July 1998 Papua New Guinea tsunami. Pure and Applied Geophysics, 160, 1969–1999.

Gerardi, F., Barbano, M.S., De Martini, P.M., Pantosti, D., 2008. Discrimination of tsunami sources (earthquake vs. landslide) on the basis of historical data in eastern Sicily and southern Calabria. Bulletin of the Seismological Society of America*,* 98 (6), 2795–2805.

Gianfreda, F., Mastronuzzi, G., Sansò, P., 2001. Impact of historical tsunamis on a sandy coastal barrier: an example from the northern Gargano coast, southern Italy. Natural Hazards and Earth System Sciences, 1, 213–219.

Goff, J., Chagué-Goff, C., Nichol, S., 2001. Paleotsunami deposits: A New Zealand perspective. Sedimentary Geology, 143, 1–6, doi: 10.1016/S0037-0738(01)00121-X.

Goff, J., McFadgen, B.G., Chagué-Goff, C., 2004. Sedimentary differences between the 2002 Easter storm and the 15th Century Okoropunga tsunami, southeastern North Island, New Zealand. Marine Geology, 204, 235–250, doi: 10.1016/S0025-3227(03)00352-9.

Goodman-Tchernov, B.N., Dey, H.W., Reinhardt E.G., McCoy F., Mart Y., 2009. Tsunami waves generated by the Santorini eruption reached Eastern Mediterranean shores. Geology, 37, 943-946.

Guidoboni, E., Comastri, A., Traina, G., 1994. Catalogue of ancient earthquakes in the Mediterranean area up to the 10th century, eds. I.N.G. and S.G.A., Bologna, Italy, 504 pp.

Jaffe, B., Gelfenbaum, G., 2002. Using tsunami deposits to improve assessment of tsunami risk. Solutions to Coastal Disasters ’02 Conference Proceedings, pp. 836–847

Jarosewich, E., Nelen, J.A., Norberg, J.A., 1980. Reference samples for electron microprobe analysis. Geostandards Newsletter, 4 (1), 43-47.

Jerome, 380. Chonicon Eusebii, Eusebius Chonicon, ed. R. Helm, GSC 47, Berlin 1956.

Kortekaas, S., Dawson, A.G., 2007. Distinguishing tsunami and storm deposits: an example from Martinhal, SW Portugal. Sedimentary Geology, 200, 208-221.
Hutchinson, I., Clague, J.C., Mathewes, R.W., 1997. Reconstructing the tsunami record on an emerging coast: a case study of Kanim Lake, Vancouver Island, British Columbia, Canada. Journal of Coastal Research 13, 545–553.
Istituto Idrografico della Marina, 1999. Carta Nautica da Capo Passero a Capo S. Croce, scala 1:100.000.
Lacisio, P., 1543. Lettera di Paolo Lacisio ad Amerbach, Strasburgo 7 marzo 1543, in: Hartmann, A. (Ed.), "Die Amerbachkorrespondens" 5, Basel 1858, 414 pp.
Lambeck, K., Antonioli, F., Purcell, A., Silenzi, S., 2004. Sea level change along the Italian coast for the past 10,000 yrs. Quaternary Science Reviews, 23, 1567–1598.
Le Bas, M.J., Le Maitre, R.W., Streckeisen, A., Zanettin, B.A., 1986. Chemical classification of volcanic rocks based on the total alkali-silica diagram. Journal of Petrology, 27, 745-750.
Lentini, F., Carbone, S., Cugno, G., Grasso, M., Scamarda, G., Sciuto, F., Montanari, L., Romeo, M., Ferrara, V., 1986. Geological map of the north-eastern Hyblean sector. Ed. S.E.L.C.A. Map scale 1:50.000, Firenze (in Italian).
Lorito, S., Tiberti, M.M., Basili, R., Piatanesi, A., Valensise, G., 2008. Earthquake-generated tsunamis in the Mediterranean Sea: Scenarios of potential threats to Southern Italy. Journal of Geophysical Research 113, B01301, doi:10.1029/2007JB004943.

Mastronuzzi, G., Sansò, P., 2000. Boulders transport by catastrophic waves along the Ionian coast of Apulia (southern Italy). Marine Geology, 170, 93-103.
Mastronuzzi, G., Sansò, P., 2004. Large boulder accumulations by extreme waves along the Adriatic coast of southern Apulia (Italy). Quaternary International, 120, 173–184.
Mastronuzzi, G., Pignatelli, C., Sansò, P., Selleri, G., 2007. Boulder accumulations produced by the 20th of February, 1743 tsunami along the coast of southeastern Salento (Apulia region, Italy). Marine Geology, 242, 191–205.
McCoy, F., Heiken, G., 2000. Tsunami generated by the Late Bronze Age eruption of Thera (Santorini), Greece. Pure and Applied Geophysics, 157, 1227–1256, doi: 10.1007/s000240050024
Minoura, K., Imamura, F., Kuran, U., Nakamura, T., Papadopoulos, G.A., Takahashi, T., Yalciner, A.C., 2000. Discovery of Minoan tsunami deposits. Geology, 28, 59–62.
Mongitore, A., 1743. Istoria cronologica de' terremoti di Sicilia, in: "Della Sicilia ricercata nelle cose più memorabili" 2, Palermo, pp. 345-445.
Morton, R.A., Gelfenbaum, G., Jaffe, B.E., 2007. Physical criteria for distinguishing sandy tsunami and storm deposits using modern examples. Sedimentary Geology, 200, 184-207.
Nanayama, F., Shigeno, K., Satake, K., Shimokawa, K., Koitabashi, S., Miyasaka, S., Ishii, M., 2000. Sedimentary differences between the 1993 Hokkaido–Nansei–Oki tsunami and the 1959 Miyakojima typhoon at Taisei, southwestern Hokkaido, northern Japan. Sedimentary Geology 135, 255–264.

Nanayama F., R. Furukawa, K. Shigeno, A. Makino, Y. Soeda and Y. Igarashi, 2007. Nine unusually large tsunami deposits from the past 4000 years at Kiritappu marsh along the southern Kuril Trench. Sedimentary Geology, 200, 275-294.

Nichol S.L., J.R. Goff, R.J.N. Devoy, C. Chague-Goff, B. Hayward and I. James, 2007. Lagoon subsidence and tsunami on the west coast of New Zealand. Sedimentary Geology, 200, 248-262.

Noormets, R., Crook, K.A.W., Felton, E.A., 2004. Sedimentology of rocky shorelines: 3. Hydrodynamics of megaclast emplacement and transport on a shore platform, Oahu, Hawaii. Sedimentary Geology 172, 41–65.

Pantosti, D., Barbano, M.S., De Martini, P.M., Smedile, A., 2008. Geological Evidence of Paleotsunamis at Torre degli Inglesi (NE Sicily). Geophysical Research Letters, 35, L05311, doi:10.1029/2007GL032935

Papazachos, B., Papazachou, C., 1997. The earthquakes of Greece, Editions Ziti, Thessaloniki, Greece, 304 pp.

Pignatelli, C., Sansò, P., Mastronuzzi, G., 2009. Evaluation of tsunami flooding using geomorphological evidence. Marine Geology 260, 6–18.

Pinegina, T.K., Bourgeois, J., 2001. Historical and paleo-tsunami deposits on Kamchatka, Russia: long-term chronologies and long-distance correlations. Natural Hazards and Earth System Sciences, 1, 177-185.

Pinegina, T.K., Bourgeois, J., Bazanova, L.I., Melekestsev, I.V., Braitseva, O.A., 2003. A millennial-scale record of Holocene tsunamis on the Kronotskiy Bay coast, Kamchatka, Russia. Quarternary Research, 59, 36-47.

Pino, N.A., Giardini, D., Boschi, E., 2000. The December 28, 1908, Messina Straits, southern Italy, earthquake: Waveform modelling of regional seismograms. Journal of Geophysical Research, 105, NO B11, 25473-25492.

Platania, G., 1909. Il Maremoto dello Stretto di Messina del 28 dicembre 1908. Bollettino della Società Sismologica Italiana, 13, 369-458.

Sabatini, V., 1910. Contributo allo studio dei terremoti calabresi. Tip. Bertero. Roma.

Sarpkaya, T., Isaacson, M., 1981. Mechanics of Wave Forces on Offshore Structures. Van Nostrand Reinhold Company Inc. 650 pp.

Scheffers, A., Kelletat, D., Vött, A., Matthias May, S., Scheffers, S., 2008. Late Holocene tsunami traces on the western and southern coastlines of the Peloponnesus (Greece). Earth and Planetary Science Letters, 269, 271-279.

Scheffers, A., Kelletat, D., 2003. Sedimentologic and geomorphologic tsunami imprints worldwide-A review. Earth-Science Reviews, 63, 83–92, doi: 10.1016/S0012-8252(03)00018-7

Scicchitano, G., Monaco, C., Tortorici, L., 2007. Large boulder deposits by tsunami waves along the Ionian coast of south-eastern Sicily (Italy). Marine Geology, 238, 75–91.

Shaw, B., Ambraseys, N.N., England, P.C., Floyd, M.A., Gorman, G.J., Higham, T.F.G., Jackson, J.A., Nocquet, J.M., Pain, C.C., Piggott M.D., 2008. Eastern Mediterranean tectonics and tsunami hazard inferred from the AD 365 earthquake. Nature Geoscience, 1, 268-276, doi: 10.1038/ngeo151 Article

Scheffers, A., Scheffers, S.R., 2007. Tsunami deposits on the coastline of West Crete (Greece). Earth and Planetary Science Letters, 259, 613–624.

Shiki, T., Tachibana, T., Fujiwara, O., Goto, K., Nanayama, F., Yamazaki, T., 2008. Characteristic features of tsunamiites. In: Shiki, T., Tsuji, Y., Yamazaki, T., Minoura, K., (Eds.), Tsunamiites - Features and Implications, pp. 319-340. Elsevier, Amsterdam.

Spirito, F., 2006. Eventi meteorologici estremi in Mediterraneo. M.Sc. thesis, University of Bologna, Italy.

Stiros S. C., 2001. The AD 365 Crete earthquake and possible seismic clustering during the fourth to sixth centuries AD in the Eastern Mediterranean: a review of historical and archaeological data. Journal of Structural Geology, 23, 545-562

Stuiver, M., Reimer, P.J., 2005. Radiocarbon calibration program CALIB REV5.0.2, copyright, available at http://calib.cub.ac.uk/calib/.

Sugawara, D., Minoura, K., Imamura, F., 2008. Tsunamis and tsunami sedimentology. In: Shiki, T., Tsuji, Y., Yamazaki, T., Minoura, K., (Eds.), Tsunamiites - Features and Implications, pp. 9-49. Elsevier, Amsterdam.

Sunamura, T., Horikawa, K., 1974. Two dimensional beach transformation due to waves. Proceedings 14th Coastal Engineering Conference. American Society of Civilian Engineers, 920–938.

Tinti, S., Maramai, A., Graziani, L., 2007. The Italian Tsunami Catalogue (ITC), Version 2. Available on-line at: http://www.ingv.it/servizi-e-risorse/BD/catalogo-tsunami/catalogo-degli-tsunami-italiani

Tuttle, M.P., Ruffman, A., Anderson, T., Jeter, H., 2004. Distinguishing tsunami from storm deposits in eastern North America: The 1929 Grand Banks tsunami versus the 1991 Halloween storm. Seismological Research Letters, 75, 117–131.